ATMOSPHERIC ENVIRONMENT: X 27 (2025) 100347

Contents lists available at ScienceDirect

Atmospheric Environment: X

journal homepage: www.journals.elsevier.com/atmospheric-environment-x

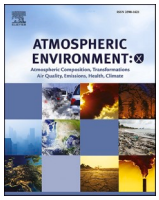

On the potential of biogeochemical models to predict hot moments of N_2O following dry-wet cycles

Lukas Hey [a,*], Katharina H.E. Meurer [b], Hermann F. Jungkunst [a]

[a] IES Landau, RPTU Kaiserslautern-Landau, Fortstr. 7, 76829 Landau, Germany
[b] Department of Soil & Environment, Swedish University of Agricultural Sciences – SLU, 75007 Uppsala, Sweden

1. Introduction

A major challenge in climate change science is to identify, model, and assess the risks of self-amplifying feedback loops between climate and terrestrial ecosystems. With climate change the risk of systems reaching tipping points due to such feedbacks increases (Kaufmann and Pretis, 2023; Lenton et al., 2019; Menon et al., 2007; Roe, 2009) and may already be unfolding.

Such is the case for the greenhouse gas (GHG) nitrous oxide (N_2O), where its recent steep rise in atmospheric concentration cannot be explained by an increase of global nitrogen fertilization alone (Griffis et al., 2017; Rychel et al., 2020; Thompson et al., 2019), suggesting self-amplification. Episodic events such as dry-wet and freeze-thaw cycles, capable of triggering peak N_2O emissions (Congreves et al., 2018) known as hot moments (McClain et al., 2003), are likely contributors to such self-amplification. Hot moments are generally triggered by rapid changes in soil water and enhanced substrate availability leading to shifts in microbial activity. Rewetting, through precipitation, irrigation or thawing reactivates microbes and under increased anaerobiosis denitrification is enhanced which triggers an emission pulse of N_2O (Congreves et al., 2018).

Recently, more attention has been paid to freeze-thaw than to dry-wet cycles due to their apparent higher potential to increase emissions (Congreves et al., 2018) and uncertainties remaining regarding their impact on N_2O emissions in the first place. While some studies associate dry-wet cycles induced hot moments rather with CO_2 emissions (Sang et al., 2022), the majority of available studies suggest, that agricultural soils rich in labile carbon (C) and reactive nitrogen (N) are capable of producing extreme N_2O emission pulses when rewetting follows extreme drying (Anthony and Silver, 2021; Barrat et al., 2020; Guo et al., 2014; Harris et al., 2021; Molodovskaya et al., 2012; Song et al., 2022). Despite their high emission potential (Anthony and Silver, 2021; Barrat et al., 2020; Guo et al., 2014), the long-term relevance of meteorological dry-wet cycle induced hot moments under climate change remains uncertain as reported contributions to annual N_2O emissions range from as little as 2 % to as high as 70 % (Zhao et al., 2011; Davidson, 1992). Yet, as current climatic changes indicate an increase in dry-wet cycles across the whole globe in the near future (Chai et al., 2021; IPCC, 2014) and N-fertilizer inputs continue to rise (Griffis et al., 2017; Aryal et al., 2022; Huang et al., 2022a), both the magnitude and frequency of such events will most likely increase as well. Assessing the potential risk of self-amplifying N_2O feedbacks from nutrient rich agricultural soils under these changing conditions is therefore critical.

Biogeochemical models are widely used to simulate soil-climate interactions and are well suited for projecting such feedbacks. However, to simulate hot moments accurately, models must capture short-term soil moisture dynamics and need to be responsive to meteorologically induced dry-wet cycles. Meaning, it is imperative to use best possible climate projections for highly likely future scenarios. However, depending on the combination of Global Circulation Model (GCM) and Regional Climate Model (RCM) and the applied post processing techniques, individual future climate projections inherit a high degree of variability and uncertainty, especially with regards to precipitation distribution and climate extremes (Iles et al., 2020; Lhotka and Kyselý, 2022; Sillmann et al., 2017). Although projection uncertainty can be reduced by using a Multi Model Ensemble (Tegegne et al., 2020; Wang et al., 2018) and by calculating the ensemble mean (Tegegne et al., 2020; Wang et al., 2018; Balhane et al., 2022), it comes with the risk of smoothing precipitation patterns and climate extremes (Tegegne et al., 2020) which are essential for robust N_2O predictions, especially in the context of dry-wet cycles.

Compounding these challenges, biogeochemical models need to perform satisfyingly under default parametrization as they are increasingly applied at larger scales (Ogle et al., 2020), where site specific parametrization is challenging and often not feasible. This makes it critical to evaluate how well models perform under default parametrization and whether they are able to capture key feedback mechanisms such as dry-wet cycle induced hot moments when driven by an ensemble

* Corresponding author.
E-mail address: lukas.hey@rptu.de (L. Hey).

https://doi.org/10.1016/j.aeaoa.2025.100347
Received 16 December 2024; Received in revised form 18 June 2025; Accepted 8 July 2025
Available online 9 July 2025

of future climate projections. Even if field and laboratory studies have yet to conclusively demonstrate how significantly such events contribute to cumulative annual emission rates.

In this study we analyzed how biogeochemical models input with climate projections respond to meteorologically induced dry-wet cycles as characterized by precipitation heterogeneity and whether they capture the potential for self-amplifying feedbacks in the form of N_2O hot moments from agricultural soils under climate change. We conducted three calculation exercises using the models CANDY, LDNDC, DNDC and DayCent within a simplified, theoretical simulation setup comparing annual N_2O emission rates and associated hot moments under default model parametrization. All biogeochemical models were driven by the same ten climate projections of the EURO-CORDEX ensemble, including the ensemble mean in the first calculation exercise.

2. Methods

2.1. Biogeochemical models

All simulation exercises were performed with the four process based-biogeochemical models CANDY v.22.6 (Carbon & Nitrogen DYnamics) (Franko et al., 1995), LDNDC v.1.35 (Landscape DeNitrification & DeComposition) (Haas et al., 2013), DNDC95 (DeNitrification & DeComposition) (Li et al., 1992a, 1992b) and DayCent17EVI (Daily CENTURY) (Parton et al., 1998). Running on daily time steps, input parameters include information about soil properties, agricultural management applications as well as daily meteorological data including precipitation, temperature (mean, min, max) and global radiation. Information about shared soil input parameters as well as management schedules can be retrieved from Table S1 and Table S2, respectively. Detailed information, manuals and supplementary materials regarding the individual biogeochemical models can be requested and or downloaded for CANDY (https://www.somod.info/candy_cdy22_intro.php), LDNDC (https://ldndc.imk-ifu.kit.edu), DNDC (https://www.dndc.sr.unh.edu). DayCent is available upon request from the developers.

2.2. Climate data and scenario development

The first calculation exercise established the baseline simulation framework using ten climate projections (Table S3) from the EURO-CORDEX ensemble (Jacob et al., 2014). These projections include daily information about minimal, maximal, and mean temperature, mean daily precipitation and surface downward solar radiation at a spatial resolution of 0.11° (~12.5 km). Stuttgart, which represents a location in between maritime and continental conditions in Germany, was selected as model-region to represent the future changes in climatic conditions. The mean regional climate consisted of the regions 08111/08115/08116/08118/08119 ('Stuttgart und angrenzende Landkreise') as described by GERICS 'Klimaausblicke für Landkreise'. The climate projections were selected based on demonstrating the smallest relative bias in mean precipitation between April and September from 1971 to 2000 compared to HYRAS (hydrometeorology gridded dataset), which served as the reference observational dataset. All multi-model ensemble projections are based on IPCC's Representative Concentration Pathway (RCP) scenario, RCP 8.5. This scenario assumes an increase of GHG emissions throughout the 21st century, resulting in an increase in radiative forcing of 8.5 W m^{-2} by the end of the century relative to its pre-industrial levels. The multi-model ensemble mean was calculated similar to Wang et al. (2018), and weighting of individual projections are assumed equal. The results from this first calculation exercise, the baseline, served as the reference for evaluating model behaviour and were used for comparison in all subsequent simulation exercises.

In the second calculation exercise, we aimed to assess the isolated impact of projected changes in precipitation patterns under climate change on simulated N_2O emissions. To achieve this, we manipulated each of the climate projections by excluding temperature development with climate change and instead fixing daily temperature values to those from year 1972 for each respective projection. This approach ensures that any variation in simulated N_2O emission patterns can be directly attributed to changes in precipitation, while also allowing an indirect assessment of temperatures effect by comparing with the baseline established in the first exercise.

For the third calculation exercise, to evaluate model performance under conditions favouring an increase in dry-wet cycles, we designed specific precipitation-free scenarios (PFS). In these scenarios, the annual precipitation sum of each year was kept constant but redistributed randomly over the year based on a defined probability that any given day could be precipitation free. For example, in PFS-10 %, approximately 10 % of the days (~35 days) are precipitation free, resulting in a relative homogeneous distribution of precipitation across the remaining 90 % of days and a low probability for dry-wet cycles. In contrast, a PFS-70 % leaves ~255 days without precipitation, concentrating the same annual precipitation on just 30 % of annual days, resulting in much more intense individual precipitation events and higher probability for changing dry-wet conditions. Increasing PFS values therefore directly correspond to an increased intensity of dry-wet cycles until a critical threshold is reached, beyond which the number of dry days exceeds the probability for dry-wet cycles to occur. We applied this approach across all ten projections with PFS values ranging from 0 % to 90 % (+-1 %) in 10 % increments.

Results from all calculation exercises were summarised and presented in 30-year intervals (2010–2039, 2040–2069, 2070–2099). In the first calculation exercise, simulated emissions were evaluated relative to a historical reference period (1980–2009). In the second and third exercise, the baseline emission trends then served as the reference for the manipulated climate simulation scenarios, as described above.

2.3. Simulation setup

In order to specifically address the influence of climate change-induced temperature and precipitation changes on simulated N_2O emissions, certain adjustments and simplifications were made to the simulation setup. The total simulation period was divided into individual simulation periods, each consisting of a three-year spin-up followed by the result year for evaluation.

During the spin-up period, meteorological data from the related result year was repeated. Further simplifications included soil profile homogenization and the annual repetition of a single agricultural management practice. Specifically, we assumed a crop rotation of winter wheat with three fertilization applications totalling 240 kg N ha^{-1} $year^{-1}$, reflecting high N fertilization levels. Expected yield was set to 7.28 t ha^{-1} as derived from the average yield data for Germany from 1995 to 2016 (Faustzahlen für die Landwirtschaft, 2018) including the yield data from 2022 (BMEL - Bundesministerium für Ernährung und Landwirtschaft). These measures aim to minimize potential C and N accumulation or loss, ensuring that changes in N_2O emissions can be attributed solely to climate change.

2.4. CANDY

CANDY (Carbon And Nitrogen DYnamics) simulates C and N dynamics with a focus on agricultural systems (Franko et al., 1995). CANDY incorporates sub-models for soil water, temperature, and crop growth. The model simulates N_2O emissions resulting from denitrification, influenced by soil temperature and water content. The soil profile is divided into 20 homogeneous layers of 10 cm thickness. Hydrological processes are modelled using the capacity (or tipping bucket) concept, allowing downward water flux only when field capacity is exceeded. Nitrogen losses occur through leaching of nitrate (NO_3^-) and gaseous emissions including ammonia volatilization and N_2O emissions, triggered by anaerobic turnover (Meurer et al., 2016). Denitrification rate

calculation involves soil moisture and temperature reduction functions, NO_3^- pool size, and carbon in the active soil organic matter pool, limited by a denitrification constant. Similar to Parton et al. (1996), dinitrogen (N_2) and N_2O are considered together during denitrification and partitioned based on factors including water filled pore space, CO_2 production, NO_3^- concentration and soil texture.

2.5. DNDC

DNDC95 simulates daily and seasonal C and N dynamics as well as GHG emissions with focus on agricultural soils in a 0–50 cm soil profile with multiple layers (Li et al., 1992a, 1992b), where the depth of each layer is determined by the saturated hydraulic conductivity (Zhang et al., 2021). The model includes submodules for soil climate, crop growth, decomposition, and denitrification, incorporating detailed soil C and N cycling. Across the soil profile, soil physical properties are assumed to be uniform with the exception of C and N pools of various layers which are logarithmically initialized using input data. The 'tipping-bucket' approach is adopted to simulate downward soil water movement which is dependent on each layer's water storage capacity such as field capacity, involving a rapid drainage of a soil layer to the next once it reaches field capacity (Parton et al., 1998). DNDC assumes the 'anaerobic balloon' concept to be applied to determine conditions and allocate substrates required for nitrification and denitrification, occurring simultaneously at aerobic and anaerobic microsites, respectively (Zhang et al., 2021). The rate of nitrification is controlled by soil temperature, moisture, pH, and nitrifier activity (Wang et al., 2021). Following the 'leaky pipe' concept described by (Stange et al., 2000), N-trace gas production during nitrification is determined by the fraction of nitrified ammonium, which varies with soil moisture, temperature, and pH. Nitrification is impacted only when water-filled pore space (WFPS) > 0.05, with a negative linear association (Wang et al., 2021). During denitrification, the DNDC model simulates the sequential reduction of NO_3^- to NO_2, NO, N_2O, and ultimately to N_2 using Michaelis-Menten kinetics and the Pirt functions (Zhang et al., 2021; Wang et al., 2021). The rate of each reduction step is determined as a function of denitrifiers, dissolved organic carbon (DOC), specific nitrogenous oxides, temperature, redox potential (Eh), and soil pH (Wang et al., 2021).

2.6. LDNDC

LDNDC, a simulation framework designed for terrestrial ecosystem models at both site and regional scales (Haas et al., 2013), originates from the site-scale model MoBiLE (Grote et al., 2009), which was developed based on the earlier models Arable-DNDC and Forest-DNDC (Li et al., 1992b, 1994; Stange et al., 2000). Its modular design allows the utilization of exchangeable sub modules including the soil-chemistry module MeTrx (Kraus et al., 2015, 2016), the plant growth model PlaMox (Kraus et al., 2016), the hydrology module WatercycleDNDC (Kiese et al., 2011) and the microclimate module CanopyECM (Grote et al., 2009). In LDNDC, the depth of the soil profile and the number of layers is flexible, and user defined. In MeTrx, nitrification is modelled as a two-stage process where ammonia is stepwise oxidised to NO_2^- and to NO_3^-. While the second step of nitrification is calculated independent of microbial biomass, the first step of nitrification depends on microbial biomass and growth rate described as a function of DOC, O_2 and NH_4^+. Here, nitrification is slightly negatively correlated with pH (Booth et al., 2005) and influenced by soil temperature and moisture (Boos et al., 2024). Microbial denitrification is calculated as a four-step process including the stepwise reduction of the nitrogen species NO_3^-, NO_2^-, NO and N_2O. The denitrification rate of each nitrogen species is determined by its relative abundance, and all denitrification steps are calculated based on the actively denitrifying microbial biomass. The activity of these microbes is regulated by a harmonic mean of soil temperature and water content dependent response coefficient. Similar to nitrification, the microbial growth rate dependents on the availability of carbon and nitrogen (Boos et al., 2024). One important feature of LDNDC is its unique capability to simulate multiple sites simultaneously, ensuring that all cells are synchronized with respect to time, which is crucial for successful model coupling (Haas et al., 2013; Klatt et al., 2016). For our simulation framework we used the soil-chemistry module MeTrx at sub daily timesteps for simulating soil carbon and N turnover, the plant growth module PlaMox and the hydrology module WatercycleDNDC at daily timesteps, respectively.

2.7. DayCent

DayCent is the daily time step version of CENTURY including submodules for plant production, soil water, soil temperature, and organic matter cycling, nitrification, denitrification, methane oxidation in upland soils, and methanogenesis in flooded systems (Parton et al., 1998; Grosso et al., 2001). The model computes daily WFPS using stored water, inputs, evapotranspiration demand, and soil properties like field capacity, wilting point, bulk density, and saturated conductivity (Parton et al., 1998). Similar to DNDC, DayCent employs the 'tipping-bucket' approach for simulating soil water movement. This method involves rapidly draining a soil layer to the next layer once it reaches field capacity, as described by Parton et al. (1998). DayCent simulates N_2O emissions from both nitrification and denitrification processes, utilizing soil WFPS as a proxy for O_2 availability to regulate their potential. Nitrification is determined by soil NH_4^+ concentration, WFPS, soil temperature, pH, and soil texture, with N_2O flux calculated as a proportion of total nitrified N (Parton et al., 2001). Nitrification is limited by soil moisture stress and O_2 availability, with optimal conditions around 50 % WFPS. Furthermore, nitrification rates decline exponentially under more acidic pH conditions and decrease with lower temperatures (Gurung et al., 2021). Denitrification is a function of soil NO_3^- concentrations, labile C availability (using soil respiration as proxy), WFPS, and soil physical properties related to soil texture affecting gas diffusivity. Soil temperature and pH do not influence denitrification rates. The denitrification rate increases exponentially with higher WFPS values, particularly when WFPS >0.6, across all soil textures (Wang et al., 2021). Initially, DayCent models denitrification as the total denitrification rate ($N_2 + N_2O$), which is then partitioned into N_2 and N_2O, considering the N_2/N_2O ratio as a function of soil NO_3^-, soil respiration, WFPS and soil texture (Wang et al., 2021). DayCent assumes no consumption of N_2O produced in deeper layers. Independent of the soil layer, once N_2O is produced it is released to the atmosphere (Xing et al., 2023).

2.8. Statistical analysis

All statistical analyses, data evaluation and visualisation was done using R version 4.2.2 (R Core Team, 2022) within the IDE RStudio version 2022.12.0.353 (Posit team, 2022) and the package *rstatix* (Kassambara, 2023). Significance testing was done by Kruskal-Wallis statistical testing following a Wilcoxon's test. Significance between groups was assumed for p-values <0.05.

'Hot moments' of N_2O emissions were identified similar to Molodovskaya et al. (2012), i.e., by applying the box plot method. Its great advantage besides its simplicity to other methods is the linkage of magnitude of the numerical event to the median and not the mean allowing its usage even for non-normal distributed data (Walfish, 2006). In this study, we used the mild approach for the upper fence (UF) calculated by the box plot method, applied over a complete year, as a primary threshold to identify N_2O peak events and potential hot moments, which has been identified as the optimal method to calculate hot moments (Stuchiner et al., 2024):

$$UF = Q3 + n(Q3 - Q1) \quad \text{(Eq. 1)}$$

The UF was calculated for each scenario and simulation year, with

Q1 as 25th percentile, Q3 as 75th percentile, and n as the fixed distance (n = 1.5). Any daily emission flux exceeding the UF was identified as a hot moment.

Calculated climate indices included dry days, dry spells, and extreme precipitation days. A dry day was assumed if daily precipitation < 1 mm, an extreme precipitation day if daily precipitation exceeded 20 mm. The identification of dry spells involved setting lower and upper boundaries for their duration. Each year was analyzed to determine the occurrence of dry spells based on these boundaries for every climate scenario. Dry spell lengths were categorized into two groups: 7–10 days and greater than 14 days.

Last but not least, if not explicitly available as model output (CANDY & LDNDC), WFPS values were calculated similar to Guo et al. (2014):

$$WFPS = \left(\frac{VSWC}{1 - \left(\frac{bd}{pd} \right)} \right) * 100 \quad \text{(Eq. 2)}$$

where *VSWC* is the volumetric soil water content [$m^3\ m^{-3}$], *bd* the bulk density [g cm^{-3}] and *pd* the particle density [g cm^{-3}].

3. Results

3.1. Baseline scenario

The trends in annual N_2O emissions relative to the reference period (dotted line) as simulated by the biogeochemical models, displayed in Fig. 1, show distinct patterns depending on the model used. Three of four models projected decreasing emissions under future climate projections, which was contrary to our initial expectations. Trends as simulated with the Climate Projection Mean (CPM) amplified the trends as observed with the Individual Climate Projections (CPI) in both increasing and decreasing directions, respectively.

CANDY projected a steady decrease in annual N_2O emissions over time (Fig. 1). While individual years and projections showed increased emissions in some outliers, the median emissions under CPI showed significant decreases ($p < 0.05$): from 19.8 % in the 2010–2039 period, to 25 % in 2040–2069, and 30.8 % in 2070–2099 relative to the reference period 1980–2010. The CPM simulations indicated a similar, yet slightly larger, decrease compared to CPI, with median decreases of 21.2 %, 31.4 %, and 43.7 % over the respective periods. Notably, emissions in all periods were significantly different between CPM and CPI ($p < 0.05$). LDNDC projected the opposite trend, with a clear increase in annual N_2O emissions over time (Fig. 1). Under CPI, median emissions increased significantly ($p < 0.05$), by 6.1 % in the first period (2010–2039), 28.9 % in 2040–2069, and 64.7 % in 2070–2099. The variance in emissions increased notably in later periods, with the largest annual outlier showing an increase of approximately 800 % relative to the reference period. CPM simulations amplified these trends, showing even larger increases of 19.9 %, 147.3 %, and 307.8 % for the three respective periods, all significantly different from CPI ($p < 0.05$). DNDC showed minimal changes in annual emissions over time. Median emissions under CPI increased slightly, but not significantly, by 0.7 % in 2010–2039, decreased by 0.3 % in 2040–2069, and increased again by 1.7 % in 2070–2099 (Fig. 1). Individual years and projections displayed occasional outliers with increased emissions compared to the reference period. CPM simulations reflected a similar trend, with small but not significant increases (with the exception for the last period) in emissions: 3.2 % in 2010–2039, 4.4 % in 2040–2069, and 10 % ($p < 0.05$) by 2070–2099. DayCent projected decreasing emissions similar to CANDY (Fig. 1). Median emissions under CPI showed significant declines ($p < 0.05$) by 4.3 % in the first period, 16 % in the second, and 30 % in the final period. CPM simulations (negatively) amplified CPI trends, though the difference between CPM and CPI was not statistically significant. Emissions with the CPM significantly decreased by 15.7 % in 2010–2039, by 18.2 % in 2040–2069 and by 38.1 % in the last period compared to the reference period.

In addition to the observed trends in N_2O emissions, the number of hot moments and their contribution to annual cumulative N_2O emissions was evaluated under baseline conditions (Table 1). For LDNDC, under CPI, the median number of identified hot moment days in the first period accounts for 10.9 % of the days in a year contributing 53 % to annual cumulative N_2O emissions (Table 2). Both the number of hot moments and their contribution to annual emission totals decreased over time. In the last period, hot moments were identified for 7.7 % of annual days, contributing 37.3 % to annual cumulative emissions (Table 1 + 2). DayCent exhibited a similar number of hot moments under baseline conditions. In the first period, the median number of hot moment days was ~11 % of a year, contributing 59.5 % to annual cumulative emissions. Like LDNDC, the number of hot moments and their contribution decreased over time, though less pronounced. By 2070–2099, 10.4 % of the days annually were identified as hot moments, contributing 53.1 % to cumulative annual N_2O emissions (Table 1 + 2). CANDY and DNDC showed significant differences in the number of simulated hot moments, both, compared to DayCent and LDNDC, and between each other. In

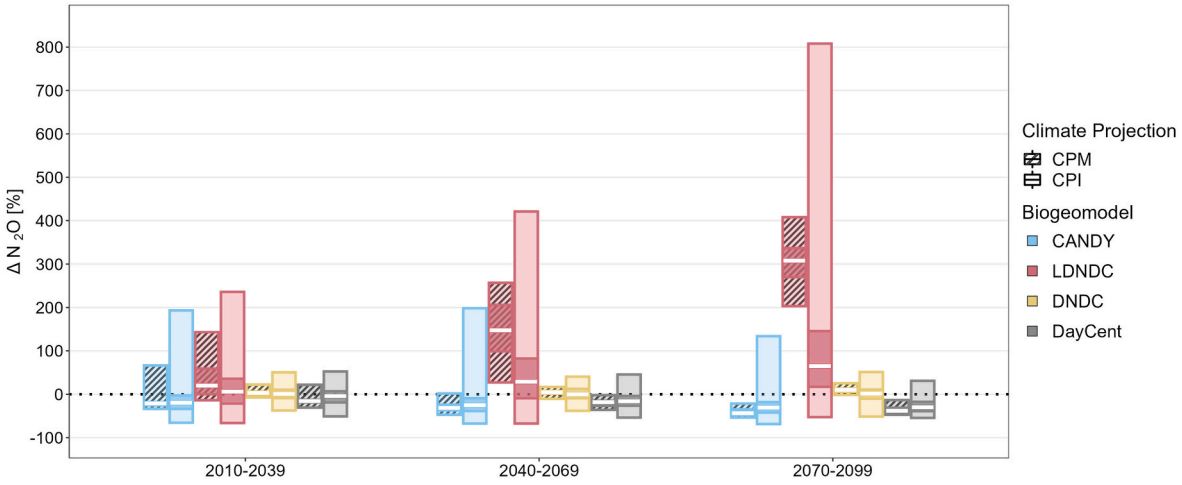

Fig. 1. Percentage change in annual N_2O emissions relative to the reference period (1980-2009) across 30-year intervals as simulated by the four biogeochemical models CANDY (blue), LDNDC (red), DNDC (yellow), and DayCent (grey). Boxplots show the range of all annual N_2O emissions under both, the climate projection mean (CPM, striped) and the ten individual climate projections (CPI, unpatterned). Upper and lower edges of the inner, saturated boxes represent the 75th and 25th percentile, while outer boxes include outliers. Median is shown as white line in the boxes.

Table 1
Median annual percentage [%] of days identified as hot moment averaged over all ten climate projections.

Treatment	CANDY			LDNDC		
	2010–2039	2040–2069	2070–2099	2010–2039	2040–2069	2070–2099
baseline (CPI)	0.0	0.0	0.0	10.9	9.9	7.7
CPM	0.0	0.0	0.0	9.6	5.7	3.0
const. temp.	0.0	0.0	0.0	13.0	12.3	10.4
0 % PFS	0.0	0.0	0.0	6.6	3.0	1.0
10 % PFS	0.0	0.0	0.0	7.1	3.8	1.4
20 % PFS	0.0	0.0	0.0	8.5	3.8	1.6
30 % PFS	0.0	0.0	0.0	7.5	5.7	2.5
40 % PFS	0.0	0.0	0.0	9.3	6.9	3.8
50 % PFS	0.0	0.0	0.0	10.7	8.2	6.0
60 % PFS	0.0	0.0	0.0	10.7	9.6	7.9
70 % PFS	0.0	0.0	0.0	11.8	10.1	8.5
80 % PFS	0.0	0.0	0.0	11.2	9.8	9.3
90 % PFS	0.0	0.0	0.0	9.0	9.0	8.0
	DNDC			**DayCent**		
	2010–2039	2040–2069	2070–2099	2010–2039	2040–2069	2070–2099
baseline (CPI)	15.9	15.3	14.0	11.0	10.7	10.4
CPM	19.9	19.7	18.3	11.5	10.8	9.4
const. temp.	15.9	15.3	15.1	11.0	10.4	9.8
0 % PFS	19.2	19.2	18.4	11.2	11.0	10.4
10 % PFS	18.4	17.8	16.7	11.2	11.0	10.4
20 % PFS	17.3	17.0	16.4	11.2	11.0	10.4
30 % PFS	17.3	16.7	15.8	11.2	11.0	10.7
40 % PFS	16.4	16.2	15.1	11.2	11.0	10.4
50 % PFS	15.9	15.3	14.5	11.5	11.2	10.7
60 % PFS	15.1	14.8	14.0	11.2	11.2	10.7
70 % PFS	14.0	13.2	12.6	11.2	11.0	10.7
80 % PFS	12.6	12.1	11.2	11.8	11.2	11.0
90 % PFS	11.8	11.0	10.4	12.1	12.3	12.0

Table 2
Median hot moment contribution [%] to annual cumulative N_2O emissions averaged over all ten climate projections.

Treatment	CANDY			LDNDC		
	2010–2039	2040–2069	2070–2099	2010–2039	2040–2069	2070–2099
baseline (CPI)	0.0	0.0	0.0	53.0	46.8	37.3
CPM	0.0	0.0	0.0	35.3	22.5	12.8
const. temp.	0.0	0.0	0.0	57.7	55.5	47.7
0 % PFS	0.0	0.0	0.0	26.7	13.1	4.7
10 % PFS	0.0	0.0	0.0	29.7	17.3	6.2
20 % PFS	0.0	0.0	0.0	35.7	18.5	7.6
30 % PFS	0.0	0.0	0.0	35.4	24.3	11.1
40 % PFS	0.0	0.0	0.0	40.9	30.2	18.1
50 % PFS	0.0	0.0	0.0	49.3	36.7	28.5
60 % PFS	0.0	0.0	0.0	51.8	45.8	37.3
70 % PFS	0.0	0.0	0.0	56.7	49.7	42.5
80 % PFS	0.0	0.0	0.0	55.8	48.9	45.3
90 % PFS	0.0	0.0	0.0	45.1	45.0	40.1
	DNDC			**DayCent**		
	2010–2039	2040–2069	2070–2099	2010–2039	2040–2069	2070–2099
baseline (CPI)	99.5	99.4	99.2	59.5	56.6	53.1
CPM	99.9	99.9	99.8	55.5	52.6	45.1
const. temp.	99.4	99.4	99.4	59.4	56.6	53.5
0 % PFS	99.8	99.8	99.8	56.7	53.8	50.9
10 % PFS	99.7	99.6	99.5	57.6	55.0	51.2
20 % PFS	99.5	99.5	99.4	58.6	56.7	52.5
30 % PFS	99.4	99.3	99.1	59.3	56.9	52.9
40 % PFS	99.2	99.2	99.0	60.7	57.4	53.1
50 % PFS	99.1	99.1	98.8	62.1	59.0	54.1
60 % PFS	99.1	99.9	98.7	62.9	60.4	56.1
70 % PFS	99.0	98.9	98.6	64.3	61.0	57.3
80 % PFS	99.0	98.9	98.5	66.6	63.2	60.5
90 % PFS	99.2	99.0	98.8	69.9	70.6	68.0

CANDY, the median number of hot moments was 0 across all periods, with hot moments identified only in outlier years and projections. In contrast, DNDC identified hot moments made up 15.9 % annually in the first period, decreasing over time, as in the other models (Table 1 + 2). However, in DNDC, the annual contribution of hot moments to cumulative N_2O emissions remained above 99 % throughout all periods, indicating that hot moments were the primary source of N_2O emissions across the entire simulation period.

Interestingly, hot moments were also observed under CPM calculations, referring values can be found in Tables 1 and 2 respectively. Overall, the emission trends in Fig. 1, along with the identified hot moments (Table 1), serve as the baseline for subsequent comparisons, including simulations with manipulated climate projections. This baseline allows us to assess the impact of individual climate change traits on N_2O emissions, as well as hot moments and their contribution to annual cumulative emissions in the following sections.

3.2. Temperature manipulation

In this calculation exercise, the exclusion of the temperature effect revealed the isolated impact of precipitation patterns on simulated N_2O emissions. Notably, three of the models (CANDY, DayCent, and DNDC) showed only marginal changes in median annual emissions when compared to the baseline scenario as seen in Fig. 2, indicating a stronger sensitivity to precipitation. LDNDC, on the other hand, demonstrated a clear downward trend in emissions under constant temperature, suggesting a stronger sensitivity to temperature changes.

Under constant temperature, CANDY showed only minor changes in emissions compared to the baseline scenario. Overall, median N_2O emissions were slightly higher, with a 5.6 % increase in 2010–2039, 9.7 % in 2040–2069, and 11.1 % in 2070–2099 relative to the baseline (Fig. 2). These increases, though small, were statistically significant ($p < 0.05$). LDNDC projected a significant decrease in emissions under constant temperature, revealing a stronger sensitivity to temperature changes. Relative to the baseline, median emissions decreased significantly ($p < 0.05$) by 15.7 % in 2010–2039, 30.3 % in 2040–2069, and 40.8 % in the last period (Fig. 2). Additionally, the variability in individual projections diminished over time, indicating a decreased difference in emissions spread in relation to the baseline, as shown by the reduced spread of outliers.

DNDC displayed only a slight reduction in emissions compared to the baseline under constant temperature as shown in Fig. 2, with median emissions decreasing significantly ($p < 0.05$) by 7.5 % in 2010–2039, 5.6 % in 2040–2069, and 8.3 % in 2070–2099. However, the spread of individual projections increased as time progressed, indicating a greater difference to respective baseline simulations in later periods. DayCent was the least affected by the temperature manipulation, showing no significant changes in emissions relative to the baseline scenario. Median emissions decreased slightly by 1.8 % in 2010–2039, increased marginally by 2.4 % in 2040–2069, and then decreased again by 2.7 % in 2070–2099.

Similar to the baseline, CANDY did not simulate any hot moments across all periods, and as a result, median hot moments did not contribute to cumulative annual N_2O emissions (Table 1 + 2). In contrast, the median contribution of hot moments to annual cumulative N_2O emissions remained above 99 % for DNDC throughout all periods, corresponding to the baseline results. LDNDC simulated number of hot moments in the first period accounted for 12.6 % of the days in a year, contributing 57.7 % to the annual cumulative N_2O emissions (Table 1 + 2). As in the baseline results, both the number of hot moments and their contribution to N_2O emissions decreased over time but remained higher in all periods under the constant temperature compared to the baseline. As shown in Tables 1 and 2, by 2070–2099 the number of hot moment days decreased to 10.4 % of a year, with their contribution to annual emissions dropping to 47.7 %. DayCent also showed a reduction in both the number of hot moment days and their contribution to annual N_2O emissions over time with similar values compared to the baseline. In the first period, ~11 % of the days were identified as hot moments, contributing 59.4 % to the annual cumulative emissions (Table 1 + 2). By 2070–2099, hot moments accounted for 9.9 % of the days and contributed 53.5 % to annual emissions.

3.3. Precipitation free scenarios

In this calculation exercise, the annual number of hot moments under increasing iterations of PFS is shown in Fig. 3, related annual cumulative N_2O emissions relative to the baseline in Fig. 4. The occurrence and trend of hot moments and their contribution to annual emissions varied considerably across the different biogeochemical models.

Most interestingly, LDNDC was the only model following the expected trend with hot moments increasing as the number of dry days increased, peaking between 70 and 80 % PFS as shown in Fig. 3. Beyond this threshold, the length of consecutive dry days reduced the frequency of dry-wet cycles and therefore the number of hot moments, resulting in their decline at 80–90 % PFS. At these peak events, hot moments made up over 11 % of days annually (Table 1) and contributed over 55 % to cumulative annual emissions in the first period (Table 2). Identified hot moments and their contribution gradually decreased over time, similar to the baseline scenario. At peak events, annual days identified as hot moments in the last period were reduced to 9 % contributing less than 46 % to annual emissions, respectively. In certain outlier years and climate projections no hot moments were detected.

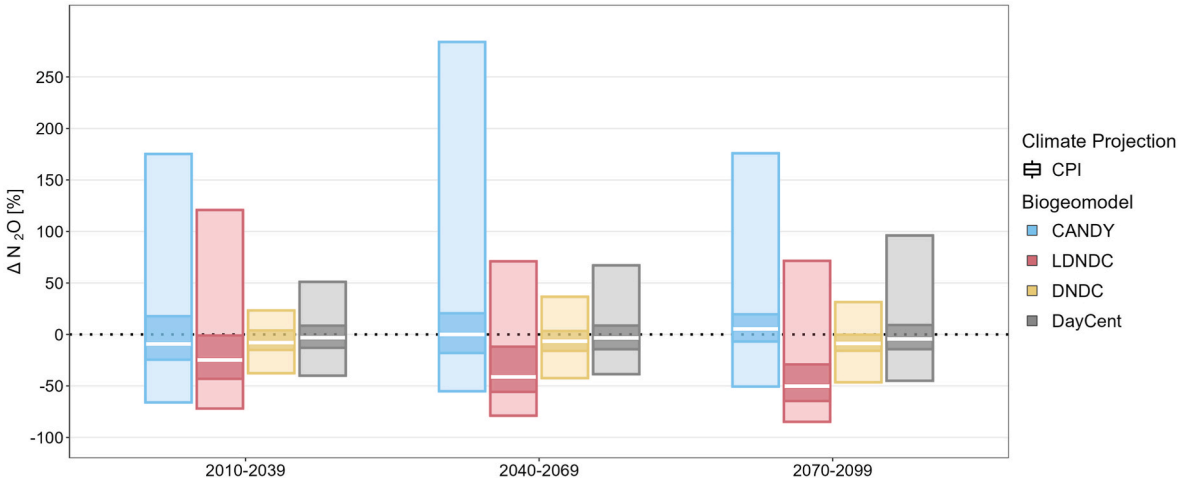

Fig. 2. Percentage change in annual N_2O emissions relative to the baseline scenario (dotted line) across 30-year intervals as simulated by the four biogeochemical models CANDY (blue), LDNDC (red), DNDC (yellow), and DayCent (grey) under temperature manipulation. The temperature profile was kept constant (by repeating the 1972 temperature profile) to isolate the effect of precipitation patterns on N_2O emissions. Boxplots show the range of all annual N_2O emissions under the ten individual climate projections (CPI, unpatterned). Upper and lower edges of the inner, saturated boxes represent the 75th and 25th percentile, while outer boxes include outliers. Median is shown as white line in the boxes.

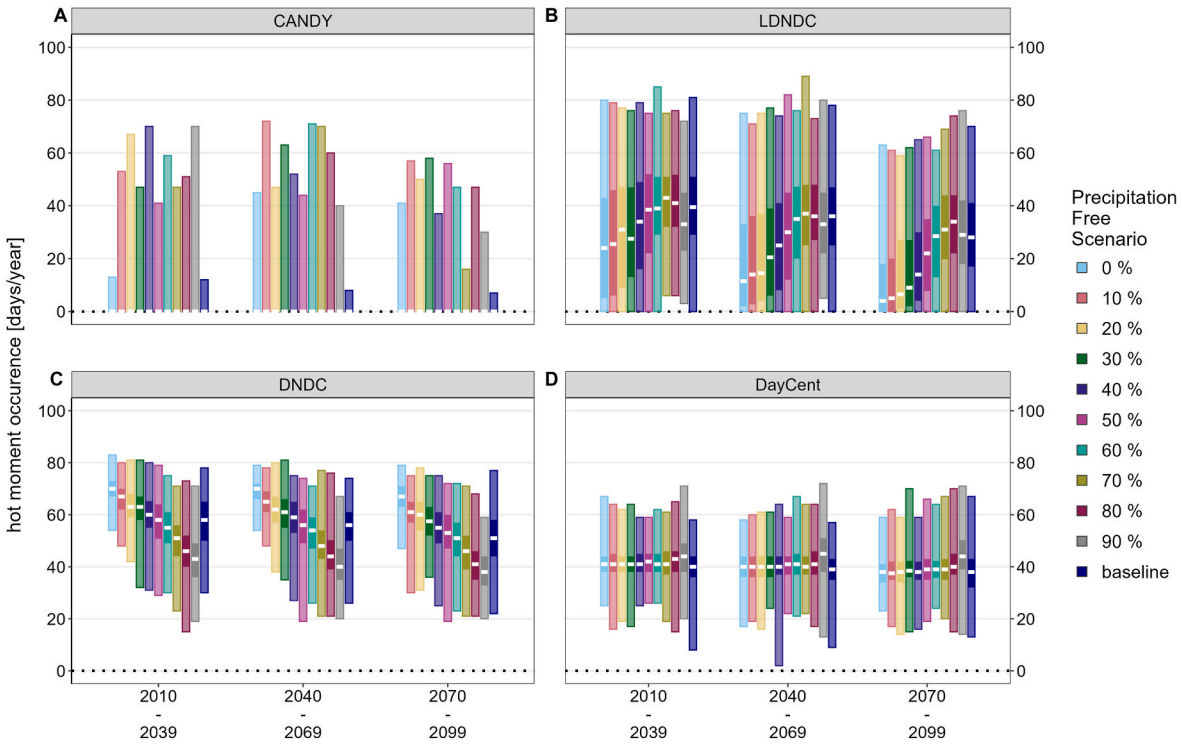

Fig. 3. Number of annual occurring hot moments for both, the baseline simulations and all iterations of PFS across 30-year intervals as simulated by the four biogeochemical models A) CANDY, B) LDNDC, C) DNDC, and D) DayCent. Precipitation Free Scenarios (PFS) were generated by randomly redistributing the annual precipitation totals for each year based on the scenario iteration value (0-90%). Higher PFS percentages indicate an increase in dry days (days with <1 mm of precipitation), followed by more intense precipitation events. The total annual precipitation amount remains the same across all PFS iterations and the baseline. Boxplots show the range of all hot moments under the ten individual climate projections. Upper and lower edges of the inner, saturated boxes represent the 75th and 25th percentile, while outer boxes include outliers. Median is shown as white line in the boxes.

With CANDY the annual median number of simulated hot moments was 0 in all periods (Table 1). Hot moments were only detectable in specific outlier years and climate projections as illustrated by the spread of the boxplots in Fig. 3. Furthermore, no clear trend on the impact of increasing iterations of PFS on the number of hot moments was observable, except for a general decrease over time. DNDC, on the other hand, exhibited a clear trend, with the number of hot moments gradually decreasing as PFS iterations increased (Fig. 3). Unlike CANDY, hot moments were identified in all years and across all climate projections. Notably, DNDC had the highest proportion of days identified as hot moments, particularly at lower PFS iterations, where hot moments accounted for nearly 20 % of the days annually (Table 1). However, regardless of the number of hot moments identified, they consistently contributed to 99 % of cumulative annual N_2O emissions across all periods and PFS iterations as shown in Table 2. DayCent maintained a relatively constant number of hot moments up to PFS-70 % in all periods, with approximately 11 % of days identified as hot moments. Interestingly, the number of hot moments did not change considerably at lower iterations of PFS compared to the baseline, as originally expected. A small increase was observed at PFS-80 %, followed by a noticeable rise at PFS-90 %, indicating that hot moments became more frequent during extreme dry periods (Fig. 3). Similar to DNDC, all years and climate projections included hot moments.

While the number of hot moments and their contribution to cumulative annual N_2O emissions varied across the PFS iterations, depending on the biogeochemical model, the overall trend in N_2O emissions was more surprising. Rather than following expected patterns, two distinctive trends in cumulative annual N_2O emissions emerged across the PFS iterations, as illustrated in Fig. 4.

Both, LDNDC and DayCent show an interesting pattern where, although the proportion of N_2O emitted during hot moments increased, the overall cumulative annual emissions steadily decreased as PFS iterations increased (Fig. 4). This suggests that while hot moments became more frequent (Fig. 3), their contributions to total annual emissions did not result in higher cumulative N_2O fluxes, indicating a decreasing trend in emissions with increasing precipitation heterogeneity (Fig. 4). Similarly, DNDC showed a gradual decline in cumulative annual emissions with increasing PFS iterations. However, in contrast to LDNDC and DayCent, DNDC's N_2O emissions were dominated by hot moments (as seen in Table 2), making them the primary contributor across all periods and climate projections. DNDC's emissions can be attributed almost entirely to hot moments, with minimal contribution from background emissions.

CANDY, on the other hand, deviated from the other models exhibiting a different trend. As shown in Fig. 4, CANDY was the only model to simulate an increase in annual median N_2O emissions as PFS iterations increased. In the first period (2010–2039), annual median emissions gradually rose until PFS-80 %, then declined with PFS-90 %. However, this decrease was not observed in later periods, where emissions continued to rise beyond PFS-80 %. Moreover, the cumulative annual N_2O emissions in CANDY simulations can be attributed to background emissions alone rather than hot moments (see Table 2), contrasting DNDC. Hot moments were detected only in outlier years (see Fig. 3).

Interestingly, CANDY projected lower cumulative N_2O emissions than the baseline scenario for PFS iterations below 80 % (Fig. 4). In contrast, LDNDC and DNDC projected higher emissions around the same PFS iterations (70–80 %). DayCent consistently simulated higher cumulative emissions than the baseline scenario in all PFS iterations, except for PFS-90 % in the first period.

3.4. N_2 emissions

N_2 emissions for all PFS iterations and the baseline are shown in Fig. 5. Unfortunately, CANDY does not output N_2 and is therefore

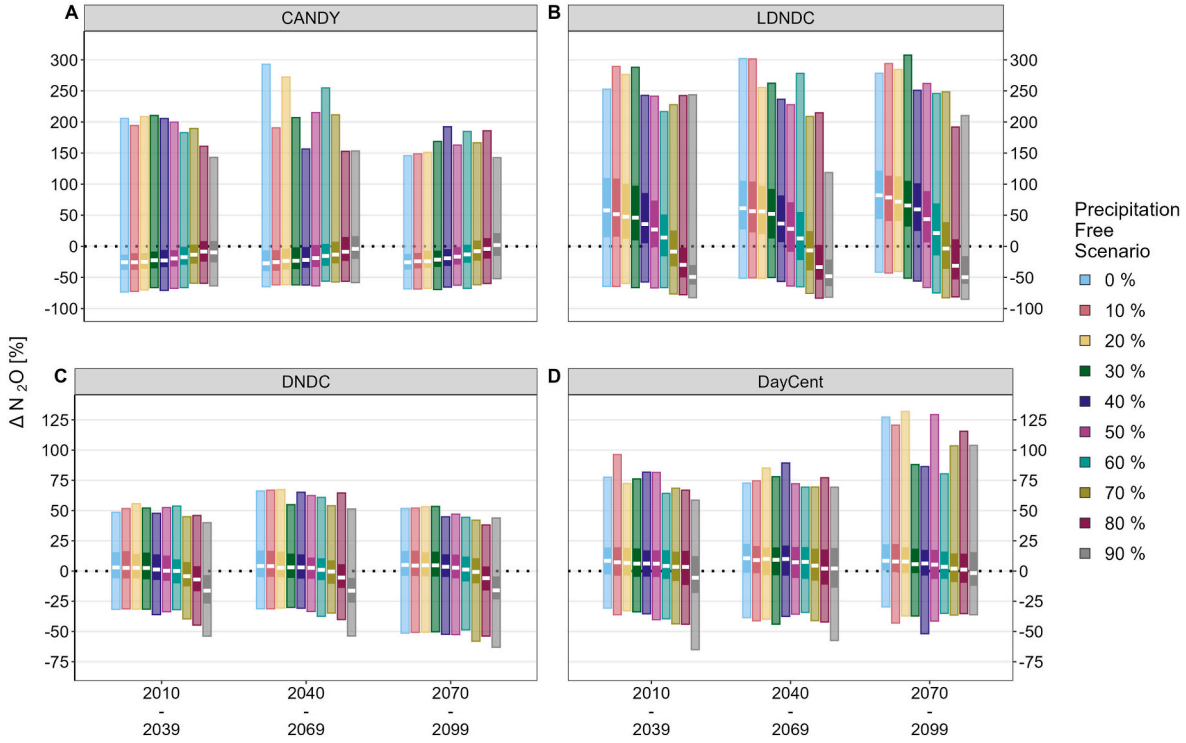

Fig. 4. Percentage change in annual N_2O emissions relative to the baseline for all iterations of PFS across 30-year intervals as simulated by the four biogeochemical models A) CANDY, B) LDNDC, C) DNDC, and D) DayCent. Precipitation Free Scenarios (PFS) were generated by randomly redistributing the annual precipitation totals for each year based on the scenario iteration value (0-90%). Higher PFS percentages indicate an increase in dry days (days with <1 mm of precipitation), followed by more intense precipitation events. The total annual precipitation amount remains the same across all PFS iterations and the baseline. Boxplots show the range of all hot moments under the ten individual climate projections. Upper and lower edges of the inner, saturated boxes represent the 75th and 25th percentile, while outer boxes include outliers. Median is shown as white line in the boxes.

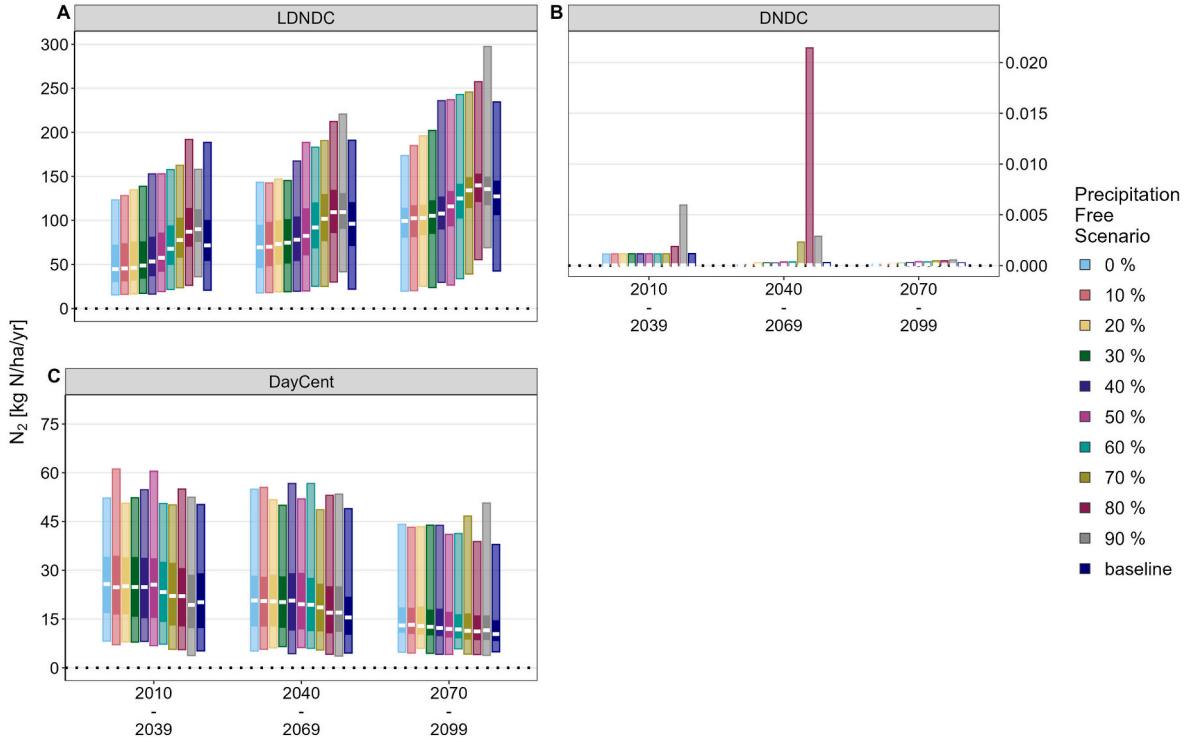

Fig. 5. Annual N_2 emissions across 30-year intervals as simulated by the three biogeochemical models A) LDNDC, B) DNDC, and C) DayCent. No N_2 output is possible with CANDY. Boxplots show the range of all annual N_2 emissions for the ten individual climate projections. Upper and lower edges of the inner, saturated boxes represent the 75th and 25th percentile, while outer boxes include outliers. Median is shown as white line in the boxes.

excluded from Fig. 5.

N_2 emissions varied considerably between the three remaining models LDNDC, DNDC, and DayCent. While LDNDC and DayCent displayed clear emission patterns, DNDC's N_2 emissions were negligibly low (below 1 kg N/ha) and were observed primarily in outlier years and projections across all PFS iterations and the baseline (see Fig. 5). Most notably, LDNDC's N_2 emissions, unlike its N_2O emissions, closely mirrored the trend associated with hot moment occurrences, as shown in Fig. 3. N_2 emissions were comparably high (median values ranging between approximately 45-150 kg N/ha), and they consistently increased with higher iterations of PFS. In the last two periods a threshold emerged at 80 % PFS, beyond which N_2 emissions began to decrease. Moreover, unlike N_2O emissions, N_2 emissions increased over time across all PFS iterations as well as the baseline. Contrary, DayCent depict much lower emissions (median emissions ranging between approx. 7–25 kg N/ha) decreasing over time for all iterations of PFS and the baseline (Fig. 5). Also, N_2 emissions show a more decreasing trend with increasing PFS iterations, similar to simulated N_2O emissions. In contrast, DayCent exhibited much lower N_2 emissions (median values ranging from approximately 7-25 kg N/ha – Fig. 5), which decreased over time across all PFS iterations and the baseline. Additionally, N_2 emissions in DayCent did show a decreasing trend with increasing PFS iterations, similar to the N_2O emissions.

3.5. Mean annual WFPS

Fig. 6 illustrates the mean annual WFPS for all PFS iterations and the baseline across the four models.

In CANDY, WFPS remained consistently high across all periods, with a slight decrease over time and across increasing PFS iterations. Median WFPS values ranged between 70 % and 80 %. The spread of boxes is more compact in the earlier periods (2010–2039), with greater variability emerging in later periods (see Fig. 6). In LDNDC, WFPS remained relatively stable across all PFS iterations, with values consistently clustering around 80 % throughout all periods. Unlike the other models, LDNDC exhibited only minimal spread of WFPS with a slightly more downward trend in variability over time. DNDC exhibited the highest annual median WFPS values out of the four models, particularly at lower PFS iterations. Median WFPS values remained close to 85–90 % in the earlier periods, decreasing slightly over time with increasing PFS iterations. DayCent showed a clear decreasing trend in WFPS over time and with increasing PFS iterations. WFPS values in DayCent gradually decrease from around 70–80 % in the first period (2010–2039) to around 65–75 % in the last period (2070–2099). DayCent exhibited the lowest annual median WFPS levels of all the models.

4. Discussion

Researchers suggest that N_2O emissions from hot moments following dry-wet cycles will become increasingly important under climate change scenarios (Barrat et al., 2020; Zhao et al., 2011). However, only few studies have actually assessed the contribution of N_2O emissions from meteorological dry-wet cycles to annual amounts. Reported contributions vary from 2 % (Davidson, 1992) to 70 % (Zhao et al., 2011) as the relative contribution of hot moments to the annual emissions do vary in both space and time. So far it is still rather speculative to assume that hot moments have any influence on the total amount of cumulative annual N_2O emissions. While it is intuitive to assume that hot moments influence both temporal variability and cumulative amounts, this has not yet been tested. Cold moments, i.e., periods of low or zero emissions may follow hot moments resulting in similar annual cumulative emission rates as by more homogenously emitted daily N_2O. If agricultural fertilizer application rates remained the same, the amounts of reactive soil nitrogen might not change significantly, which in turn could lead to similar amounts of annually released N_2O. Nevertheless, this still remains a knowledge gap, and we are not aware of any scientific articles reporting on this.

To determine whether hot moments simply increase the

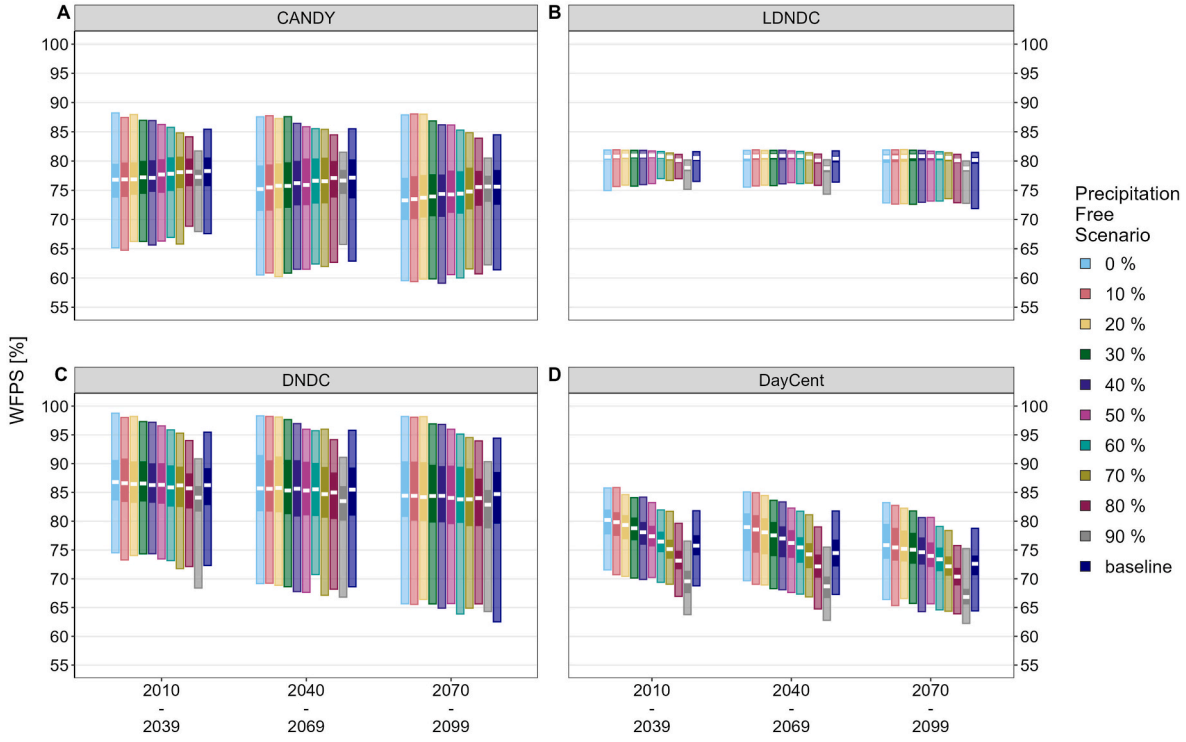

Fig. 6. Mean annual Water Filled Pore Space (WFPS) [%] across 30-year intervals as simulated by the four biogeochemical models A) CANDY, B) LDNDC, C) DNDC, and D) DayCent. Boxplots show the range of all annual N_2 emissions for the ten individual climate projections. Upper and lower edges of the inner, saturated boxes represent the 75th and 25th percentile, while outer boxes include outliers. Median is shown as white line in the boxes.

heterogeneity of daily emission rates throughout a year or actually increase total cumulative annual N_2O emissions, controlled precipitation manipulation experiments are essential. In practice, both climate and soil management often vary, making it challenging to distinguish climate from management effects on N_2O emissions. To generate accurate projections of potential self-amplifying effects between climate change-induced precipitation changes and N_2O emissions from agricultural soils, model ensembles, rather than individual models, are needed to simulate daily emission rates including hot and cold moments. However, this makes the testing of possible individual ensemble members a necessity prior to their application. If precipitation-induced hot moments prove irrelevant for annual emissions, the models could maintain their current level of simplicity.

4.1. Baseline scenario

In our first calculation exercise to establish the baseline, only one out of four models projected increasing annual N_2O emissions due to climate change (Fig. 1). As a result, the expectations of many authors were not met (Griffis et al., 2017; Aryal et al., 2022; Huang et al., 2022a; Grant and Pattey, 2008). However, rising annual emissions are anticipated not solely due to climate change, but in combination with increasing nitrogen applications. In our simulation framework we kept fertilizer levels steady over time, setting focus on climate change impact. Therefore, unchanged or even declining annual emission rates, as predicted by the other three models are comprehensible, as warmer and wetter conditions might lead to increased N losses as leachate, by runoff, increased plant uptake or stimulated soil microbes.

However, a main question will be if hot moments actually increase cumulative annual N_2O amounts or simply mirror the heterogeneity in precipitation patterns as long as the N input remains the same. According to the model study presented by Zhang et al. (2021), precipitation heterogeneity significantly elevated N_2O emissions. Their study showed that less frequent but high intense precipitation increased emissions, while more frequent but less intense patterns reduced them, especially under high fertilization treatments. Our model experiment did not confirm this. Contrary, homogenization of precipitation resulted in higher annual cumulative emissions compared to more irregular precipitation events by most models (see Fig. 4). This becomes particularly evident considering the homogenized precipitation of the CPM (Fig. 1), characterized by a homogeneous distribution due to the averaging process. The more homogeneous precipitation distribution enhanced the N_2O trends that emerged with the CPI in each of the models, heavily skewing the annual values into a positive or negative direction.

To assess model response in simulating hot moments we can examine the annual percentage of days identified as hot moments and their contribution to cumulative annual N_2O emissions (see Tables 1 and 2), although studies on this topic are limited. According to Molodovskaya et al. (2012), hot moment emissions of N_2O accounted for up to 51 % of total cumulative annual N_2O emissions, even though these events comprised less than 7 % of the total observation period days. More recently, Stuchiner et al. (2024), using the same methodology as Molodovskaya et al. (2012) which is also employed in this study, found that hot moments, on average, accounted for about 66 % of cumulative annual N_2O emissions occurring on just about 9 % of annual days.

For this study's baseline scenario, averaged across all periods and climate projections, LDNDC simulated hot moments for 9.49 $\pm$ 1.43 % days of a year contributing about 44 $\pm$ 6.52 % to annual emissions (Tables 1 and 2). Similarly, DayCent simulated that hot moments occur on 11 $\pm$ 0.25 % of annual days and accounted for about 56 $\pm$ 2.64 % of cumulative annual emissions, both falling well within the reported ranges. In CANDY, averaged over all climate projections and periods, days identified as hot moments only made up less than 0.1 % of a year with a similar low contribution to cumulative annual emissions. The reason behind this are high background emissions, shifting hot moment identifying thresholds considerably upwards. On the opposite, cumulative annual N_2O emissions with DNDC were >99 % the result of hot moments with basically no contribution of background emission. These results clearly suggest that both CANDY and DNDC show difficulties in accurately simulating hot moments under set conditions.

Based on these observations, two critical points emerge from the baseline-scenario calculations. First, we cannot assert that hot moments are exclusively due to dry-wet cycles, given that simulations with the CPM simulated hot moments as well, where dry-wet cycles are unlikely due to the very homogeneous precipitation distribution. However, the lower frequency and contribution of hot moments under CPM compared to the baseline—especially in LDNDC—alongside the seasonal occurrence patterns of such events (mainly in spring to summer and early autumn, Tables S4–S7) strongly suggest that dry-wet cycles did play a significant role contributing to hot moment occurrence. Second, not only did three of the four models show declining trends in annual N_2O emissions (see Fig. 1), which might be realistic as stated above, but all models consistently simulated a decrease in hot moment occurrence over time (Fig. 3). These trends might be linked to two key factors: (1) projections of the EURO-CORDEX ensemble which are known to overestimate precipitation amounts (Demory et al., 2020; Vautard et al., 2021) and (2) our simulation setup assuming a homogeneous soil profile have influenced simulation results. Especially in combination, these two factors might significantly influence the dry-wet cycle probability and annual emission trends and the overall simulation behaviour of models. Moreover, it can be assumed that under these conditions an increase in NO_3^- leaching is likely. This is true for CANDY and DayCent (Fig. S2), yet topsoil NO_3^- remained abundant across all models (Fig. S3), aligning with the initial simulation setup that focused primarily on the impact of climate. These two points made it necessary to manipulate the climate to unravel the impact of dry-wet cycle hot moments on cumulative annual N_2O emissions.

4.2. Temperature manipulation

To exclude the temperature effect from the precipitation effect, air temperature was kept as projected for the year 1972, thus removing the influence of climate change-related temperature shifts. This ensured that any observed hot moments would be predominantly influenced by precipitation patterns without the increasing temperature effect inherent to climate change.

Interestingly, hardly any significant effect was shown with this manipulation experiment in three of four models as seen in Fig. 2. LDNDC, which calculated increasing N_2O emissions for the combined effect of temperature increase and changes in precipitation in the baseline scenario, showed that this increase is reduced by about 30 % (averaged over all projections and periods) if temperature does not increase. The latter fits to the finding of Elli et al. (2022), who reported strong reactions of simulated N_2O emissions to both manipulated temperatures and precipitation (heterogeneity) but only minor reactions to precipitation alone. While increasing temperatures significantly affected the magnitude of the trend with LDNDC, this had comparably reduced effects on annual cumulative emissions with CANDY, DNDC and DayCent. This temperature insensitivity on annual cumulative N_2O emissions seems unlike the common consensus. While some studies attribute more impact to temperature (Huang et al., 2022a), it is commonly agreed on that the combinatory effect of precipitation and temperature lead to elevated, not decreasing N_2O emissions (Grant and Pattey, 2008; Elli et al., 2022; Huang et al., 2022b; Duan et al., 2019). The observed declining trend of cumulative annual N_2O emissions in CANDY, DNDC and DayCent, may be linked to some sort of temperature insensitivity in the models. At least for DayCent, this lies directly in the model structure, as it, for example, does not consider the impacts of soil temperature on denitrification (Wang et al., 2021). The same is true for CANDY, which, for description of the denitrification process, shares algorithms with DayCent. Improvements in this regard would greatly benefit simulation

prediction robustness, especially in the context of climate change. Nevertheless, all models did show a great sensitivity to precipitation.

Identified hot moments at constant projected temperature followed the trend of the baseline scenario, with the difference of increasing annual occurrence and contribution in LDNDC, while slightly lower in DayCent (see Tables 1 and 2). Simulations with CANDY and DNDC again were showing fewer hot moments as demonstrated already with baseline simulations (s.a.). However, though not as pronounced as in LDNDC, days identified as hot moments and their contribution to annual cumulative N_2O emissions did increase slightly compared to the baseline in these models as well. Therefore, a negative effect of increasing temperature with rising precipitation heterogeneity on the occurrence of hot moments seems likely. Yet, the decrease in the amount of identified hot moments with progressing time, as observed with the baseline simulations, prevailed. However, since the decreasing trend over time is greater than the negative effect of temperature increases on the occurrence of hot moments (at least for LDNDC, CANDY and DNDC) it leaves precipitation in either annual totals or heterogeneity as the responsible parameter for the declining trends of hot moments.

4.3. *Precipitation manipulation – hot moments and related N_2O emissions*

As stated above, the climate projections used in this study did not fully meet the criteria necessary to evaluate the impact of dry-wet cycles due to their tendency to overestimate precipitation. This limitation necessitated to manipulate towards increasing precipitation heterogeneity to force dry-wet cycles to occur more frequently. We hypothesized that this manipulation would lead to more frequent hot moments, which would, in turn, increase cumulative annual N_2O emissions until a tipping point is reached. Such tipping points are crossed when dry days exceed the stimulatory effect of dry-wet cycles and hinder N-mineralization, nitrification and hence denitrification more than fostering it, hence leading to a decrease in emissions again. Our expectations are based on Barrat et al. (2020) and Guo et al. (2014), who demonstrated that the magnitude of a hot moment and N_2O emissions in substrate-rich environments are directly linked to the difference between the dry and wet state of the soil, particularly through changes in WFPS.

Contrary to our expectations, the models did not simulate an increase in annual cumulative N_2O emissions (Fig. 4) with increasing precipitation heterogeneity, despite the rising number of hot moments (Fig. 3). While the relative contribution to annual cumulative N_2O emissions increased with increasing numbers of hot moments at each iteration of precipitation-free days (PFS), the annual cumulative emission totals decreased in respective models.

Since the quality of the individual models simulating hot moments has already been established with the baseline scenario, it is reasonable to assume that these quantities serve as indicators for the quality of the PFS simulation results. Yet, surprisingly, these manipulations highlighted possible shortcomings in how models simulate hot moments in the context of dry-wet cycles characterized by precipitation heterogeneity. At 0 % PFS, where dry-wet cycles are unlikely to occur, DayCent simulated nearly the same number of hot moments and contribution to annual N_2O emissions as the baseline scenario (see Tables 1 and 2), suggesting that a considerable portion of DayCent's simulated hot moments are likely not the product of dry-wet cycles. In contrast, LDNDC simulations at 0 % PFS did show a clear decrease in the number of hot moments compared to the baseline, indicating that the model more accurately associates hot moments with dry-wet cycles. Moreover, the expected tipping point where the number of hot moments decreases due to the limited occurrence of dry-wet cycles at higher iterations of PFS was reached in LDNDC but not in DayCent. Nevertheless, it can be concluded that the simulated hot moments in our calculation exercises show that an increasing number of modelled hot moments do not result in higher cumulative annual N_2O emissions.

As expected, the relative contribution of hot moments to annual cumulative N_2O emissions increased with increasing precipitation heterogeneity and associated dry-wet cycle intensity at respective PFS iterations across all models (Table 2). This agrees well with the principles governing this process. Barrat et al. (2020) stated that the degree of rewetting and the resulting WFPS significantly influenced N_2O emissions to the fact that larger differences between dry and wet states of the soil are leading to larger hot moments. Whereas under similar but constant anaerobicity and WFPS, emissions were much lower. Similarly, Wei et al. (2023) stated that prevailing saturated, anoxic conditions rather lead to N_2O consumption than emission, which they attribute to the low diffusivity of gases under saturated conditions. Under such conditions the N_2O diffusion to the soil surface is reduced promoting the reduction of N_2O to N_2 through denitrification. Highest N_2O flux was found below 10 % (±2 %) O_2 concentration, indicating that suboxic soil conditions are optimal to stimulate soil N_2O production in the soil while simultaneously allowing the diffusion to the soil surface, which in Wei et al. (2023) was consistent at the inflection point of 56 % WFPS. Comparably, Vor et al. (2003) showed unleashed N_2O emissions during dynamically changing low O_2 conditions (around 0–5 %), strongly indicating that changing low, not static O_2 conditions favor N_2O emissions. Soil O_2 was found to strongly inversely correlate with N_2O emissions (Song et al., 2019, 2022; Wei et al., 2023), with WPFS as a regulator limiting soil aeration and diffusivity, highlighting the sensitive balance between WFPS, O_2 availability and substrate that regulates denitrification.

In our simulation framework three of the models simulate N_2 emissions and in all of them, WFPS is the main factor determining the distribution of available N into N_2O and eventually N_2, thus determining whether nitrification or denitrification dominates. In DayCent, denitrification is driven by WFPS, serving as a proxy for O_2 availability along with labile C (e^- donor) and NO_3^- (e^- acceptor) concentrations. The threshold at which nitrification or denitrification occur depends on soil texture: while coarse-textured soils are assumed to have a higher gas diffusivity until WFPS exceeds 80 %, denitrification occurs much easier in fine-textured soils and at WFPS of ~60 %. Denitrification is calculated in a separate sub-model (Parton et al., 1996; Del Grosso et al., 2000), which first calculates the total N gas flux, i.e. $N_2 + N_2O$, using a N_2:N_2O ratio function to then split the total flux into its individual components. The ratio in turn depends on the soil gas diffusivity and the ratio of NO_3^- to labile C (i.e., the ratio of e^- acceptor to e^- donor).

Similarly, DNDC calculates denitrification in a specific sub-model, which is activated at every precipitation event and immediately upon saturation of the soil with water. It is assumed that oxic (nitrification) and anoxic (denitrification) conditions occur simultaneously in the soil controlled by the soil redox potential (Zhang et al., 2015). Like in DayCent, soluble carbon and NO_3^- are used by denitrifiers as e^- donor and acceptor, respectively (Li et al., 1992a), and determine the relative growth rates of NO_3^-, NO_2-, NO and N_2O denitrifiers. Both N_2O and N_2 are highly sensitive to the annual precipitation, soil pH, mean annual temperature, as well as the SOC content (Li et al., 1992a). Diffusion rates are calculated separately for N_2O and N_2 based on soil porosity and clay content.

While LDNDC inherits the modelling of soil temperature and moisture from DNDC, the dynamics of nitrifiers and denitrifiers that stimulate nitrification and decomposition processes follow the work presented by (Blagodatsky and Richter, 1998; Blagodatsky et al., 1998). Diffusion rates are calculated by Fick's first law (Zhang et al., 2015) – which differs from the approach used in DNDC. Equations and parameters related to denitrification are the same for both models (see (Zhang et al., 2015)).

It can be concluded that all models in this study relied heavily on soil NO_3^- and WFPS, and in turn on precipitation events to simulate denitrification products. Throughout our simulation exercises, topsoil NO_3^- was abundant in all models, and mean annual WFPS values were within the optimal range for denitrification. Despite these favorable conditions, total N_2O emissions decreased with increasing precipitation heterogeneity in three of the models. This phenomenon mirrors the behaviour

already observed in the baseline scenario with the CPM, where median N_2O emissions in LDNDC, DayCent, and DNDC were elevated under more homogeneous precipitation distributions (see Fig. 1). Interestingly, this agrees with findings from Miller et al. (2022), where projected future precipitation patterns for the U.S upper Midwest did not significantly affect growing-season N_2O emissions, but were instead favoured by optimal soil WFPS and N concentrations. Similarly, Barrat et al. (2020) stated that it is well established that saturated soils are more likely to produce N_2O. However, this contradicts their earlier claim (s.a.) and findings from several other studies, that increased N_2O emission can be associated with the intensification of precipitation (Huang et al., 2022a; Jiao et al., 2024; Li et al., 2020; Yan et al., 2018; Zhang et al., 2022) up to a certain threshold at which the precipitation intensity exceeds the stimulatory effect on emission rates (Li et al., 2023).

The decline in N_2O emissions with increasing precipitation heterogeneity and dry-wet cycles in LDNDC can be attributed to a shift in the balance between N_2O and N_2 production towards N_2. As shown in the results (Fig. 5), LDNDC's simulated N_2 emissions increased with more hot moments, almost mirroring their trend, resulting in a significant release of N_2 emissions especially compared to the other models. Inspecting WFPS values, the elevated denitrification rate becomes more apparent, as median annual WFPS values (Fig. 6) just slightly exceeded the optimal range for N_2O emissions at 65–80 % (Dobbie and Smith, 2001; Gillam et al., 2008). Additionally, median daily WFPS distributions across all projections showed that values rarely surpassed 75–85 % (Figs. S4–S6), even during summer under the highest iteration of PFS. These prolonged elevated WFPS values probably shifted the N_2:N_2O ratio in favor of N_2. However, compared to the other models, LDNDC's simulated daily WFPS values appear visibly higher than for the other models.

In contrast, DayCent showed decreasing N_2O and N_2 emissions despite the denitrification fostering conditions, i.e., optimal median annual WFPS and NO_3^- levels. Unlike LDNDC, median daily WFPS values in DayCent showed a notable 'belly' (dropping WFPS values – Figs. S4–S6) in summer. However, outliers never fell below 46 % or exceeded 95 % resulting in sharp WFPS changes in spring and autumn, suggesting some sort of WFPS value capping within the model algorithms. Still, denitrification emission products decreased throughout all simulation scenarios, suggesting another factor to be responsible.

DNDC, on the other hand, displayed highly elevated mean annual WFPS values compared to the other models, likely overestimating soil saturation. Unlike LDNDC, DNDC did show a very pronounced 'summer-belly' (Figs. S4–S6), i.e. a drop in WFPS over the summer, yet this drop occurred after returning from a very wet winter at 100 % WFPS. The model's denitrification sub-model considers the transformation of denitrification products during their diffusion through the soil matrix, which would help explain the near absence of N_2O background emission. Yet, N_2 emissions were negligible at most and almost exclusively observable in outliers, indicating that another disturbing factor might be responsible for DNDC's unique emission behaviour throughout the simulation framework.

CANDY deviated from the other models, showing increasing N_2O emissions with increasing precipitation heterogeneity. However, as established earlier, these emissions were linked to CANDY's higher emphasis on background emissions and not hot moments. Unfortunately, no N_2 emissions data was available for CANDY, making a full assessment of its denitrification behaviour difficult. Compared to the other models, CANDY's simulated median daily WFPS appeared the most 'realistic,' showing a similar curve to DNDC, but without the significantly elevated WFPS values during winter (Figs. S4–S6).

While LDNDC exhibited the expected behaviour in terms of both, increasing annual N_2O emissions over time and simulating hot moments, the simulated decrease in N_2O emissions with increasing precipitation heterogeneity can be explained by an increased denitrification rate, shifting emissions towards N_2. However, none of the other models (DayCent, DNDC, or CANDY) could attribute the observed decreases in N_2O emissions over time or across all PFS iterations to temperature or precipitation distribution alone. DayCent, despite the denitrification fostering conditions did not show increasing emissions either over time or at increasing PFS iterations. Both, DNDC and CANDY, either displayed little to no background emissions with only hot moments or vice versa. All models displayed comparably elevated median annual WFPS values to varying degrees with DayCent and LDNDC exhibiting particular distinctive anomalies in regard to their daily WFPS distribution. It is sensitive to assume that models did struggle with the elevated precipitation projected by the EURO-CORDEX ensemble, likely enhanced by the simulation setup assuming homogeneous soil conditions.

Since the simulation framework is grounded on testing models under default parametrization, it can be assumed that all models were initially parameterized and validated under much lower annual precipitation totals than those provided by the climate projections. Moreover, DayCent showed significantly elevated trace gas emissions compared to the other models, particularly N_2O (Table S7). This overestimation is likely due to the model's assumption that once N_2O is produced, it is released to the atmosphere regardless of soil layer depth (Xing et al., 2023). Under saturated conditions, limited gas diffusivity would normally inhibit N_2O escape, promoting its consumption in deeper soil layers rather than its emission (Wei et al., 2023; Goldberg et al., 2008; Kuang et al., 2019).

Therefore, to achieve accurate soil N_2O emission estimates, especially in the context of dry-wet cycles, both soil WFPS and soil O_2 levels must be considered. While soil O_2 is the primary regulator of soil N_2O concentrations (Song et al., 2019, 2022), WFPS is crucial for predicting soil surface emissions as it significantly influences gas diffusivity and soil aeration (Del Grosso et al., 2000; Klefoth et al., 2014). As established above, soil moisture alone cannot account for dynamic changes in oxygen availability caused by the addition of, for example, organic residues, manures, or N-fertilizers (Wei et al., 2023). Moreover, soil moisture does not account for small-scale O_2 concentration gradients, such as sub-anaerobic conditions, which can trigger nitrifier denitrification (Wei et al., 2023; Burgin and Groffman, 2012; Liptzin et al., 2011).

Nevertheless, the estimation accuracy can be greatly improved by considering soil O_2 status as the primary regulator of soil N_2O concentrations, along with WFPS to control gas diffusivity and subsequent surface emission. Especially in the simulation of dry-wet cycle associated hot moments. That is why the concept of the 'anaerobic balloon,' as integrated into DNDC, is a compelling approach to capture these dynamics. The balloon 'swells' under anoxic conditions, promoting substrate allocation to anaerobic microsites and enhancing denitrification. Conversely, under more oxic conditions, the balloon 'shrinks,' reducing substrate availability for denitrification and favoring nitrification. Unfortunately, this concept is highly sensitive to elevated precipitation levels, as observable from our simulations, which likely led to an over-inflated anaerobic balloon, contributing to the model's behavior under our simulation setup.

4.4. Climate projections

The goal of this study was to test biogeochemical model reactions to increasing drying and rewetting cycles. However, projections of the EURO-CORDEX ensemble as used in this study, proved to overestimate precipitation amounts and were generally too wet, which seems to be a known issue (Iles et al., 2020; Demory et al., 2020; Vautard et al., 2021). This evidently shows in the comparison with observed weather from two climate stations from the selected model region (Fig. S1 and Tables S8 and S9). Since not only the emissions of N_2O occurring in the field, but also the biogeochemical models simulating it being very sensitive to climate variability, weather data input is an important component influencing the extent to which emission simulations are biased. To overcome this shortcoming we manipulated precipitation, showing that biogeochemical models are not that well prepared and react either over-

or under sensitive to elevated precipitation. That is why the simulations framework will need to be tested with lower annual precipitation amounts and, moreover, with different soil types to verify our findings.

The internal variability, different forcing scenarios and the different responses of the projecting climate models lead to a high degree of uncertainty in the simulated climate projections (Dalelane et al., 2018), cascading down to impact studies (Wang et al., 2018). That is why climate modelers stress that climate projections are precisely that, projections of possible climatic developments, not forecasts (Cannon et al., 2020). However, this is exactly what policy makers require. Future weather forecasts that are as realistic as possible and how they drive N_2O simulations in order to develop robust and sustainable mitigation strategies. Nonetheless, due to the high uncertainty of relying on just one projection, it is emphasized to use a multi-model ensemble approach in impact studies (Tegegne et al., 2020; Wang et al., 2018). By using a multi-model ensemble, we rely on a variety of possible climate projections which cover a high variance of possible trends. Therefore, model weighting approaches such as the Model Mean approach can help to reduce the uncertainty of an ensemble significantly (Balhane et al., 2022). Nevertheless, such weighting methods can introduce unwanted side effects, especially when dealing with daily precipitation data. Due to the averaging process, climatic extreme values are not extracted (Tegegne et al., 2020) thereby possibly skewing output downstream. This unwanted introduction of bias is very evident within our results, especially in simulations with CANDY and LDNDC. Depending on the biogeochemical model, the CPM (Climate Projection Mean) heavily amplified or attenuated the simulated trend of the CPI (Individual Climate Projections). Fortunately, this is seldomly done in impact studies and most studies rely on the multi model mean of the individual projections (averaging the output - CPI), thereby reflecting the variability of the individual projections in the output.

Furthermore, current climate modelers emphasize the importance of post processing, or bias adjusting, climate projections before their utilization in impact models (Cannon et al., 2020; Chen et al., 2021; Dinh and Aires, 2023). As GCMs and RCMs often have systematic errors, such as an overestimation of rainy days or an underestimation of extremes events (Iles et al., 2020; Lhotka and Kyselý, 2022; Sillmann et al., 2017), bias adjusting aims to approximate simulated values closer to the observed data. However, the large number of available bias adjustment methods of varying complexity poses a challenge for impact modelers, who are responsible to select the most suitable approach. Due to the inherent complexity and the immense workload it entails, many impact studies either overlook or deliberately omit this step, making results disputable. Conversely, this leads to 'blindly' applying bias adjustment methods or already bias adjusted projections, without considering whether such adjustments even improve model performance or are appropriate for the study applied (Benestad et al., 2021). Bias adjusting should always be considered as a statistical post processing method missing physical arguments and applying may introduce new uncertainties (Benestad et al., 2021). In our case, we did not bias adjust the climate projections used. Commonly applied bias adjustment methods are based on the quantile mapping approach (Piani et al., 2010) which provide notable improvements for seasonal means and percentiles. Yet, they do not directly account for time-dependent statistics such as consecutive dry-wet days (Benestad et al., 2021), the evaluation of which was a main focus of this study.

4.5. Generalizability

Overall, the biogeochemical models used within this study certainly have the potential to represent expected emission patterns and trends with climate change, particularly after extensive parameterization and calibration using available measurement data on specific sites are feasible. Notably so, Del Grosso et al. (2019) demonstrated significant improved performance of DayCent after site-specific calibration and validation compared to default parametrization. However, even under good calibration, daily estimates and peak events can be over- or underestimated (Gaillard et al., 2018; Fuchs et al., 2020), which is related to unrepresented processes within the models themselves, such as freeze-thaw and rewetting dynamics (Iqbal et al., 2018). More so, parametrization becomes increasingly challenging, the greater the scale of the simulation scenario. Trade-offs need to be made between data availability and calibration accuracy. Especially in regions where regular direct measurements are scarce, models need to perform under default parametrization. As highlighted within this study, there is great potential to improve on unrepresented processes like dry-wet cycle dynamics. The biogeochemical models CANDY, DNDC, LDNDC and DayCent under default parametrization expressed very mixed results capturing expected trends under increasing dry-wet cycles. Since such biogeochemical models are increasingly applied within grand scale projects (Klatt et al., 2016; Butterbach-Bahl et al., 2022; Kraus et al., 2022; Meurer et al., 2019) and for national inventories (EPA, 2024), the challenge of achieving simulation accuracy without site-specific calibration possibilities further highlights the need to improve on unrepresented processes. Obviously, that requires a better understanding of these processes before they can be incorporated as algorithms into the models. This is currently particularly stressed for freeze-thaw cycles but is also needed for dry-wet cycles. Contemporary biogeochemical modelers apparently see the need to include freeze-thaw dynamics more than dry-wet cycles. They are believed to yield higher potentials for extraordinary cumulative annual N_2O emissions resulting from hot moments than dry-wet cycles do (Congreves et al., 2018). And notably so, DayCent developers already incorporated a version featuring freeze-thaw dynamics showing improvement of N_2O estimates applied at national scale (Del Grosso et al., 2022). Similarly, significant progress has been made to improve DNDC to better represent freeze-thaw dynamics (Del Grosso et al., 2022; Cui and Wang, 2019; Dutta et al., 2018; Yadav and Wang, 2021). Yet, while freeze-thaw dynamics are crucial in regions experiencing regular episodes of frost, it is important to note, that dry-wet cycles are more widespread across diverse climates, making them equally, if not more relevant for consideration. As climatic conditions shift towards fewer regions experiencing severe episodes of frost and more regions experiencing drying tendencies (Chai et al., 2021; Berg et al., 2016), the influence of dry-wet cycles becomes increasingly significant. The combination of climate change and increased use of N fertilisers in many regions of the world makes it clear that the potential risk of ever-increasing N_2O feedback loops is imminent.

However, in the end, the ability of models to predict biogeochemical cycling ultimately relies on the quantity and quality of data available for parametrization and validation (Berardi et al., 2020). Field and laboratory studies are in dear need to finally unravel the mysteries of these missing links. Studies need to focus on high frequency, long term measurements, capturing the spatio-temporal variability of N_2O emissions. This all plays together in order to improve our simulation estimates helping to find sustainable GHG mitigation strategies paving the way for a brighter tomorrow.

4.6. Potential improvements to the simulation setup

Certain improvements to the current simulation setup might be better suited to explore the N_2O simulation behaviour of models in the context of dry-wet cycles. Considering a heterogeneous instead of a homogeneous soil profile could significantly improve the overall simulation behaviour, as it was suspected to have greatly biased output depending on the biogeochemical model used. In this context, different soil textures need to be considered in future studies. While the used soil texture served well as a proof of concept, it limited our total understanding of the simulation behaviour. It is well established that different soil textures considerably affect N_2O relevant parameters, not only in nature but also in biogeochemical models simulating it, and the likelihood of dry-wet cycles to occur in the first place. In addition to that, we need either climate projections that robustly anticipate dry-wet cycles or

improved precipitation manipulation scenarios to more precisely depict these cycles. Future studies should not only consider periods of dry days as indicators of dry-wet cycles but also evaluate soil state variables and other measures, such as the Standardized Precipitation Index (SPI) or Standardized Precipitation Evaporation Index (SPEI), to define periods of drought. This turned out to be crucial, as in our study, we were not able to link hot moments to dry-wet cycles with absolute certainty, despite the specialized simulation setup. With these improvements, it will be possible to robustly pinpoint the exact behaviour of biogeochemical models in response to dry-wet cycle-induced hot moments.

5. Conclusions

In this study, we investigated in a simplified simulation setup the response of contemporary biogeochemical models to anticipated increases in dry-wet cycles under climate change, with a focus on their impact on N_2O emissions. Our results highlight major uncertainties in the regard of precipitation heterogeneity driven dry-wet cycle induced hot moments of N_2O, not only in areas of biogeochemical modelling but also climate projections.

It remains uncertain whether total annual rates over multi-year periods will be increased via hot moment contribution. According to our model simulations, dry-wet cycle associated hot moments will not lead to the expected increase in cumulative annual N_2O emissions and, consequently, do not appear to trigger an uncontrolled self-amplifying effect. However, it is premature to draw definitive conclusions at this stage. Not only are model improvements in regards of dry-wet cycles necessary, but future studies evaluating biogeochemical models will need to adjust on the simulation setup.

If precipitation-induced hot moments prove irrelevant for annual emissions, the models could maintain their current level of simplicity. However, they are mandatory at the daily scale to assess best management practices and help to find mitigation strategies. Presently, it is important to determine if the recent rise in atmospheric N_2O concentrations indicates that annual emissions are indeed influenced by such cycles.

A common goal within the scientific community is to make models applicable more casually without the need of extensive parametrization. Particularly in political context models will be needed to be representative substitute for measured values. To achieve this goal enhancing model algorithms is necessary, requiring comprehensive multi-year studies to better understand the long-term impacts of dry-wet cycles on N_2O emissions.

CRediT authorship contribution statement

Lukas Hey: Writing – original draft, Visualization, Software, Methodology, Investigation, Formal analysis, Data curation, Conceptualization. **Katharina H.E. Meurer:** Writing – review & editing, Supervision, Conceptualization. **Hermann F. Jungkunst:** Writing – review & editing, Supervision, Project administration, Funding acquisition, Conceptualization.

Declaration of generative AI and AI-assisted technologies in the writing process

During the preparation of this work the author(s) used ChatGPT in order to improve the quality of the English language writing. After using this tool/service, the author(s) reviewed and edited the content as needed and take(s) full responsibility for the content of the published article.

Declaration of competing interest

The authors declare that they have no known competing financial interests or personal relationships that could have appeared to influence the work reported in this paper.

Acknowledgements

The authors thank Uwe Franko for the valuable assistance with all CANDY inquiries and David Kraus (KIT-Campus Alpin) for any questions related to LDNDC. We would also like to thank Diana Rechid and Susanne Pfeifer from the Climate Service Center Germany (GERICS) for kindly providing the climate projections and their support in addressing related inquiries.

Appendix A. Supplementary data

Supplementary data to this article can be found online at https://doi.org/10.1016/j.aeaoa.2025.100347.

Data availability

Data will be made available on request.

References

Anthony, T.L., Silver, W.L., 2021. Hot moments drive extreme nitrous oxide and methane emissions from agricultural peatlands. Glob. Change Biol. 27, 5141–5153. https://doi.org/10.1111/gcb.15802.

Aryal, B., Gurung, R., Camargo, A.F., Fongaro, G., Treichel, H., Mainali, B., Angove, M.J., Ngo, H.H., Guo, W., Puadel, S.R., 2022. Nitrous oxide emission in altered nitrogen cycle and implications for climate change. Environ. Pollut. 314, 120272. https://doi.org/10.1016/j.envpol.2022.120272.

Balhane, S., Driouech, F., Chafki, O., Manzanas, R., Chehbouni, A., Moufouma-Okia, W., 2022. Changes in mean and extreme temperature and precipitation events from different weighted multi-model ensembles over the northern half of Morocco. Clim. Dyn. 58, 389–404. https://doi.org/10.1007/s00382-021-05910-w.

Barrat, H.A., Evans, J., Chadwick, D.R., Clark, I.M., Le Cocq, K., Cardenas, L.M., 2020. The impact of drought and rewetting on N2O emissions from soil in temperate and mediterranean climates. Eur. J. Soil Sci. 72, 2504–2516. https://doi.org/10.1111/ejss.13015.

Benestad, R., Buonomo, E., Gutiérrez, J.M., Haensler, A., Hennemuth, B., Illy, T., Jacob, D., Keup-Thiel, E., Katragkou, E., Kotlarski, S., Nikulin, G., Otto, J., Rechid, D., Remke, T., Sieck, K., Sobolowski, S., Szabó, P., Szépszó, G., Teichmann, C., Vautard, R., Weber, T., Zsebeházi, G., 2021. Guidance for EURO-CORDEX climate projections data use; Version1.1 - 2021.02. https://euro-cordex.net/imperia/md/content/csc/cordex/guidance_for_euro-cordex_climate_projections_data_use_2021-02_1_.pdf. (Accessed 18 March 2024).

Berardi, D., Brzostek, E., Blanc-Betes, E., Davison, B., DeLucia, E.H., Hartman, M.D., Kent, J., Parton, W.J., Saha, D., Hudiburg, T.W., 2020. 21st-century biogeochemical modeling: challenges for Century-based models and where do we go from here? GCB Bioenergy 12, 774–788. https://doi.org/10.1111/gcbb.12730.

Berg, A., Findell, K., Lintner, B., Giannini, A., Seneviratne, S.I., van den Hurk, B., Lorenz, R., Pitman, A., Hagemann, S., Meier, A., Cheruy, F., Ducharne, A., Malyshev, S., Milly, P.C.D., 2016. Land–atmosphere feedbacks amplify aridity increase over land under global warming. Nat. Clim. Change 6, 869–874. https://doi.org/10.1038/nclimate3029.

Blagodatsky, S.A., Richter, O., 1998. Microbial growth in soil and nitrogen turnover: a theoretical model considering the activity state of microorganisms. Soil Biol. Biochem. 30, 1743–1755. https://doi.org/10.1016/S0038-0717(98)00028-5.

Blagodatsky, S.A., Yevdokimov, I.V., Larionova, A.A., Richter, J., 1998. Microbial growth in soil and nitrogen turnover: model calibration with laboratory data. Soil Biol. Biochem. 30, 1757–1764. https://doi.org/10.1016/S0038-0717(98)00029-7.

Boos, C., Butterbach-Bahl, K., Denk, T., Fuchs, K., Grote, R., Haas, E., Havermann, F., Kiese, R., Klatt, S., Kraus, D., Lioba, M., Nadal Sala, D., Petersen, K., Wolf, B., 2024. LandscapeDNDC models description. https://ldndc.imk-ifu.kit.edu/products/ldndc-models-description.pdf. (Accessed 20 March 2024).

Booth, M.S., Stark, J.M., Rastetter, E., 2005. Controls on nitrogen cycling in terrestrial ecosystems: a synthetic analysis of literature data. Ecol. Monogr. 75, 139–157. https://doi.org/10.1890/04-0988.

Burgin, A.J., Groffman, P.M., 2012. Soil O2 controls denitrification rates and N2O yield in a riparian wetland. J. Geophys. Res. Biogeosciences 117. https://doi.org/10.1029/2011JG001799.

Butterbach-Bahl, K., Kraus, D., Kiese, R., Mai, V.T., Nguyen, T., Sander, B.O., Wassmann, R., Werner, C., 2022. Activity data on crop management define uncertainty of CH4 and N2O emission estimates from rice: a case study of Vietnam. J. Plant Nutr. Soil Sci. 185, 793–806. https://doi.org/10.1002/jpln.202200382.

Cannon, A.J., Piani, C., Sippel, S., 2020. Chapter 5 - bias correction of climate model output for impact models. In: Sillmann, J., Sippel, S., Russo, S. (Eds.), Clim. Extrem. their Implic. Impact Risk Assess. Elsevier, pp. 77–104. https://doi.org/10.1016/B978-0-12-814895-2.00005-7.

Chai, R., Mao, J., Chen, H., Wang, Y., Shi, X., Jin, M., Zhao, T., Hoffman, F.M., Ricciuto, D.M., Wullschleger, S.D., 2021. Human-caused long-term changes in global

aridity. Npj Clim. Atmospheric Sci. 4, 1–8. https://doi.org/10.1038/s41612-021-00223-5.
Chen, J., Arsenault, R., Brissette, F.P., Zhang, S., 2021. Climate change impact studies: should we bias correct climate model outputs or post-process impact model outputs? Water Resour. Res. 57, e2020WR028638. https://doi.org/10.1029/2020WR028638.
Congreves, K.A., Wagner-Riddle, C., Si, B.C., Clough, T.J., 2018. Nitrous oxide emissions and biogeochemical responses to soil freezing-thawing and drying-wetting. Soil Biol. Biochem. 117, 5–15. https://doi.org/10.1016/j.soilbio.2017.10.040.
Cui, G., Wang, J., 2019. Improving the DNDC biogeochemistry model to simulate soil temperature and emissions of nitrous oxide and carbon dioxide in cold regions. Sci. Total Environ. 687, 61–70. https://doi.org/10.1016/j.scitotenv.2019.06.054.
Dalelane, C., Früh, B., Steger, C., Walter, A., 2018. A pragmatic approach to build a reduced regional climate projection ensemble for Germany using the EURO-CORDEX 8.5 ensemble. J. Appl. Meteorol. Climatol. 57, 477–491. https://doi.org/10.1175/JAMC-D-17-0141.1.
Davidson, E.A., 1992. Pulses of nitric oxide and nitrous oxide flux following wetting of dry soil: an assessment of probable sources and importance relative to annual fluxes. Ecol. Bull. 149–155.
Del Grosso, S.J., Parton, W.J., Mosier, A.R., Ojima, D.S., Kulmala, A.E., Phongpan, S., 2000. General model for N2O and N2 gas emissions from soils due to dentrification. Glob. Biogeochem. Cycles 14, 1045–1060. https://doi.org/10.1029/1999GB001225.
Del Grosso, S.J., Ogle, S.M., Nevison, C., Gurung, R., Parton, W.J., Wagner-Riddle, C., Smith, W., Winiwarter, W., Grant, B., Tenuta, M., Marx, E., Spencer, S., Williams, S., 2022. A gap in nitrous oxide emission reporting complicates long-term climate mitigation. Proc. Natl. Acad. Sci. 119, e2200354119. https://doi.org/10.1073/pnas.2200354119.
Demory, M.-E., Berthou, S., Fernández, J., Sørland, S.L., Brogli, R., Roberts, M.J., Beyerle, U., Seddon, J., Haarsma, R., Schär, C., Buonomo, E., Christensen, O.B., Ciarlò, J.M., Fealy, R., Nikulin, G., Peano, D., Putrasahan, D., Roberts, C.D., Senan, R., Steger, C., Teichmann, C., Vautard, R., 2020. European daily precipitation according to EURO-CORDEX regional climate models (RCMs) and high-resolution global climate models (GCMs) from the high-resolution model intercomparison project (HighResMIP). Geosci. Model Dev. (GMD) 13, 5485–5506. https://doi.org/10.5194/gmd-13-5485-2020.
Dinh, T.L.A., Aires, F., 2023. Revisiting the bias correction of climate models for impact studies. Clim. Change 176, 140. https://doi.org/10.1007/s10584-023-03597-y.
Dobbie, K.E., Smith, K.A., 2001. The effects of temperature, water-filled pore space and land use on N2O emissions from an imperfectly drained gleysol. Eur. J. Soil Sci. 52, 667–673. https://doi.org/10.1046/j.1365-2389.2001.00395.x.
Duan, P., Song, Y., Li, S., Xiong, Z., 2019. Responses of N2O production pathways and related functional microbes to temperature across greenhouse vegetable field soils. Geoderma 355, 113904. https://doi.org/10.1016/j.geoderma.2019.113904.
Dutta, B., Grant, B.B., Congreves, K.A., Smith, W.N., Wagner-Riddle, C., VanderZaag, A. C., Tenuta, M., Desjardins, R.L., 2018. Characterising effects of management practices, snow cover, and soil texture on soil temperature: model development in DNDC. Biosyst. Eng. 168, 54–72. https://doi.org/10.1016/j.biosystemseng.2017.02.001.
Elli, E.F., Ciampitti, I.A., Castellano, M.J., Purcell, L.C., Naeve, S., Grassini, P., La Menza, N.C., Moro Rosso, L., de Borja Reis, A.F., Kovács, P., Archontoulis, S.V., 2022. Climate change and management impacts on soybean N fixation, soil N mineralization, N2O emissions, and seed yield. Front. Plant Sci. 13. https://doi.org/10.3389/fpls.2022.849896.
EPA, 2024. Draft Inventory of U.S. Greenhouse Gas Emissions and Sinks: 990-2022. U.S. Environmental Protection Agency. EPA 430-D-24-001. https://www.epa.gov/ghgemissions/draft-inventory-us-greenhouse-gas-emissions-and-sinks-1990-2022. (Accessed 18 March 2024).
Faustzahlen Für Die Landwirtschaft, fifteenth ed., 2018. KTBL, Darmstadt.
Franko, U., Oelschlägel, B., Schenk, S., 1995. Simulation of temperature-, water- and nitrogen dynamics using the model CANDY. Ecol. Model. 1–3, 213–222.
Fuchs, K., Merbold, L., Buchmann, N., Bretscher, D., Brilli, L., Fitton, N., Topp, C.F.E., Klumpp, K., Lieffering, M., Martin, R., Newton, P.C.D., Rees, R.M., Rolinski, S., Smith, P., Snow, V., 2020. Multimodel evaluation of nitrous oxide emissions from an intensively managed grassland. J. Geophys. Res. Biogeosciences 125, e2019JG005261. https://doi.org/10.1029/2019JG005261.
Gaillard, R.K., Jones, C.D., Ingraham, P., Collier, S., Izaurralde, R.C., Jokela, W., Osterholz, W., Salas, W., Vadas, P., Ruark, M.D., 2018. Underestimation of N2O emissions in a comparison of the DayCent, DNDC, and EPIC models. Ecol. Appl. 28, 694–708. https://doi.org/10.1002/eap.1674.
Gillam, K.M., Zebarth, B.J., Burton, D.L., 2008. Nitrous oxide emissions from denitrification and the partitioning of gaseous losses as affected by nitrate and carbon addition and soil aeration. Can. J. Soil Sci. 88, 133–143. https://doi.org/10.4141/CJSS06005.
Goldberg, S.D., Knorr, K.-H., Gebauer, G., 2008. N2O concentration and isotope signature along profiles provide deeper insight into the fate of N2O in soils. Isotopes Environ. Health Stud. 44, 377–391. https://doi.org/10.1080/10256010802507433.
Grant, R.F., Pattey, E., 2008. Temperature sensitivity of N2O emissions from fertilized agricultural soils: mathematical modeling in ecosys. Glob. Biogeochem. Cycles 22. https://doi.org/10.1029/2008GB003273.
Griffis, T.J., Chen, Z., Baker, J.M., Wood, J.D., Millet, D.B., Lee, X., Venterea, R.T., Turner, P.A., 2017. Nitrous oxide emissions are enhanced in a warmer and wetter world. Proc. Natl. Acad. Sci. 114, 12081–12085. https://doi.org/10.1073/pnas.1704552114.
Grosso, Del, Parton, W.J., Mosier, A.R., Hartman, M., Brenner, J., Ojima, D., Schimel, D., 2001. Simulated Interaction of Carbon Dynamics and Nitrogen Trace Gas Fluxes Using the DAYCENT Model, pp. 303–332. https://doi.org/10.1201/9781420032635.ch8.
Grosso, S.J.D., Ogle, S.M., Parton, W.J., Nevison, C., Smith, W., Gran, B., Tenuta, M., Hartman, M.D., Blanc-Betes, E., DeLucia, E.H., 2019. Modelling denitrification and N2O emissions from fertilised cropping systems using daycent. Proceedings of the Workshop on "Climate Change, Reactive Nitrogen, Food Security and Sustainable Agriculture" 15-16 April, 2019Clim. Change.
Grote, R., Lavoir, A.-V., Rambal, S., Staudt, M., Zimmer, I., Schnitzler, J.-P., 2009. Modelling the drought impact on monoterpene fluxes from an evergreen mediterranean forest canopy. Oecologia 160, 213–223. https://doi.org/10.1007/s00442-009-1298-9.
Guo, X., Drury, C., Yang, X., Reynolds, D., Fan, R., 2014. The extent of soil drying and rewetting affects nitrous oxide emissions, denitrification, and nitrogen mineralization. Soil Sci. Soc. Am. J. 78, 194–204. https://doi.org/10.2136/sssaj2013.06.0219.
Gurung, R.B., Ogle, S.M., Breidt, F.J., Williams, S., Zhang, Y., Del Grosso, S.J., Parton, W. J., Paustian, K., 2021. Modeling ammonia volatilization from urea application to agricultural soils in the DayCent model. Nutr. Cycl. Agroecosystems 119, 259–273. https://doi.org/10.1007/s10705-021-10122-z.
Haas, E., Klatt, S., Frohlich, A., Kraft, P., Werner, C.R., Kiese, R., Grote, R., Breuer, L., Butterbach-Bahl, K., 2013. LandscapeDNDC: a process model for simulation of biosphere–atmosphere–hydrosphere exchange processes at site and regional scale. https://hdl.handle.net/10568/34447. (Accessed 18 March 2024).
Harris, E., Diaz-Pines, E., Stoll, E., Schloter, M., Schulz, S., Duffner, C., Li, K., Moore, K.L., Ingrisch, J., Reinthaler, D., Zechmeister-Boltenstern, S., Glatzel, S., Brüggemann, N., Bahn, M., 2021. Denitrifying pathways dominate nitrous oxide emissions from managed grassland during drought and rewetting. Sci. Adv. 7, eabb7118. https://doi.org/10.1126/sciadv.abb7118.
Huang, Y., Ciais, P., Boucher, O., Wang, Y.-P., Tian, H., Zhou, F., Chang, J., Li, Z., Goll, D. S., Langenfelds, R., Shi, H., Pan, N., Hu, H.-W., Lam, S.K., Dong, N., 2022a. Increasing sensitivity of terrestrial nitrous oxide emissions to precipitation variations. Environ. Res. Clim. 1, 025010. https://doi.org/10.1088/2752-5295/aca2d1.
Huang, J., Liu, R., Wang, Q., Gao, X., Han, Z., Gao, J., Gao, H., Zhang, S., Wang, J., Zhang, L., Xia, X., 2022b. Climate factors affect N2O emissions by influencing the migration and transformation of nonpoint source nitrogen in an agricultural watershed. Water Res. 223, 119028. https://doi.org/10.1016/j.watres.2022.119028.
Iles, C.E., Vautard, R., Strachan, J., Joussaume, S., Eggen, B.R., Hewitt, C.D., 2020. The benefits of increasing resolution in global and regional climate simulations for European climate extremes. Geosci. Model Dev. (GMD) 13, 5583–5607. https://doi.org/10.5194/gmd-13-5583-2020.
IPCC, 2014. Climate change 2014: synthesis report. Contribution of working groups I, II and III to the fifth assessment report of the intergovernmental panel on climate change. https://www.ipcc.ch/report/ar5/syr/. (Accessed 18 March 2024).
Iqbal, J., Necpalova, M., Archontoulis, S.V., Anex, R.P., Bourguignon, M., Herzmann, D., Mitchell, D.C., Sawyer, J.E., Zhu, Q., Castellano, M.J., 2018. Extreme weather-year sequences have nonadditive effects on environmental nitrogen losses. Glob. Change Biol. 24, e303–e317. https://doi.org/10.1111/gcb.13866.
Jacob, D., Petersen, J., Eggert, B., Alias, A., Christensen, O.B., Bouwer, L.M., Braun, A., Colette, A., Déqué, M., Georgievski, G., Georgopoulou, E., Gobiet, A., Menut, L., Nikulin, G., Haensler, A., Hempelmann, N., Jones, C., Keuler, K., Kovats, S., Kröner, N., Kotlarski, S., Kriegsmann, A., Martin, E., van Meijgaard, E., Moseley, C., Pfeifer, S., Preuschmann, S., Radermacher, C., Radtke, K., Rechid, D., Rounsevell, M., Samuelsson, P., Somot, S., Soussana, J.-F., Teichmann, C., Valentini, R., Vautard, R., Weber, B., Yiou, P., 2014. EURO-CORDEX: new high-resolution climate change projections for European impact research. Reg. Environ. Change 14, 563–578. https://doi.org/10.1007/s10113-013-0499-2.
Jiao, P., Yang, L., Li, Z., Zheng, P., Nie, X., 2024. Soil type and wetting intensity control the enhancement extent of N2O efflux in soil with drought and rewetting cycles. Int. Soil Water Conserv. Res. 12, 137–144. https://doi.org/10.1016/j.iswcr.2023.05.007.
Kassambara, A., 2023. Rstatix: pipe-friendly framework for basic statistical tests. https://cran.r-project.org/web/packages/rstatix/index.html. (Accessed 21 March 2024).
Kaufmann, R.K., Pretis, F., 2023. An empirical estimate for the snow albedo feedback effect. Clim. Change 176, 107. https://doi.org/10.1007/s10584-023-03572-7.
Kiese, R., Heinzeller, C., Werner, C., Wochele, S., Grote, R., Butterbach-Bahl, K., 2011. Quantification of nitrate leaching from German forest ecosystems by use of a process oriented biogeochemical model. Environ. Pollut. 159, 3204–3214. https://doi.org/10.1016/j.envpol.2011.05.004.
Klatt, S., Kraus, D., Rahn, K.-H., Werner, C., Kiese, R., Butterbach-Bahl, K., Haas, E., 2016. Parameter-induced uncertainty quantification of regional N2O emissions and NO3 leaching using the biogeochemical model LandscapeDNDC. In: Synth. Model. Greenh. Gas Emiss. Carbon Storage Agric. For. Syst. Guide Mitig. Adapt. John Wiley & Sons, Ltd, pp. 149–171. https://doi.org/10.2134/advagricsystmodel6.2013.0001.
Klefoth, R.R., Clough, T.J., Oenema, O., Van Groenigen, J.-W., 2014. Soil bulk density and moisture content influence relative gas diffusivity and the reduction of Nitrogen-15 nitrous oxide. Vadose Zone J. 13. https://doi.org/10.2136/vzj2014.07.0089 vzj2014.07.0089.
Kraus, D., Weller, S., Klatt, S., Haas, E., Wassmann, R., Kiese, R., Butterbach-Bahl, K., 2015. A new LandscapeDNDC biogeochemical module to predict CH4 and N2O emissions from lowland rice and upland cropping systems. Plant Soil 386, 125–149. https://doi.org/10.1007/s11104-014-2255-x.
Kraus, D., Weller, S., Klatt, S., Santabárbara, I., Haas, E., Wassmann, R., Werner, C., Kiese, R., Butterbach-Bahl, K., 2016. How well can we assess impacts of agricultural land management changes on the total greenhouse gas balance (CO2, CH4 and N2O) of tropical rice-cropping systems with a biogeochemical model? Agric. Ecosyst. Environ. 224, 104–115. https://doi.org/10.1016/j.agee.2016.03.037.

Kraus, D., Werner, C., Janz, B., Klatt, S., Sander, B.O., Wassmann, R., Kiese, R., Butterbach-Bahl, K., 2022. Greenhouse gas mitigation potential of alternate wetting and drying for rice production at national scale—A modeling case study for the Philippines. J. Geophys. Res. Biogeosciences 127, e2022JG006848. https://doi.org/10.1029/2022JG006848.

Kuang, W., Gao, X., Tenuta, M., Gui, D., Zeng, F., 2019. Relationship between soil profile accumulation and surface emission of N2O: effects of soil moisture and fertilizer nitrogen. Biol. Fertil. Soils 55, 97–107. https://doi.org/10.1007/s00374-018-01337-4.

Lenton, T.M., Rockström, J., Gaffney, O., Rahmstorf, S., Richardson, K., Steffen, W., Schellnhuber, H.J., 2019. Climate tipping points — too risky to bet against. Nature 575, 592–595. https://doi.org/10.1038/d41586-019-03595-0.

Lhotka, O., Kyselý, J., 2022. Precipitation–temperature relationships over Europe in CORDEX regional climate models. Int. J. Climatol. 42, 4868–4880. https://doi.org/10.1002/joc.7508.

Li, C., Frolking, S., Frolking, T.A., 1992a. A model of nitrous oxide evolution from soil driven by rainfall events: 1. Model structure and sensitivity. J. Geophys. Res. 97, 9759–9776. https://doi.org/10.1029/92JD00509.

Li, C., Frolking, S., Frolking, T.A., 1992b. A model of nitrous oxide evolution from soil driven by rainfall events: 2. Model applications. J. Geophys. Res. Atmospheres 97, 9777–9783. https://doi.org/10.1029/92JD00510.

Li, C., Frolking, S., Harriss, R., 1994. Modeling carbon biogeochemistry in agricultural soils. Glob. Biogeochem. Cycles 8, 237–254. https://doi.org/10.1029/94GB00767.

Li, L., Zheng, Z., Wang, W., Biederman, J.A., Xu, X., Ran, Q., Qian, R., Xu, C., Zhang, B., Wang, F., Zhou, S., Cui, L., Che, R., Hao, Y., Cui, X., Xu, Z., Wang, Y., 2020. Terrestrial N2O emissions and related functional genes under climate change: a global meta-analysis. Glob. Change Biol. 26, 931–943. https://doi.org/10.1111/gcb.14847.

Li, L., Hao, Y., Wang, W., Biederman, J.A., Zheng, Z., Wang, Y., Tudi, M., Qian, R., Zhang, B., Che, R., Song, X., Cui, X., Xu, Z., 2023. Effects of extra-extreme precipitation variability on multi-year cumulative nitrous oxide emission in a semiarid grassland. Agric. For. Meteorol. 343, 109761. https://doi.org/10.1016/j.agrformet.2023.109761.

Liptzin, D., Silver, W.L., Detto, M., 2011. Temporal dynamics in soil oxygen and greenhouse gases in two humid tropical forests. Ecosystems 14, 171–182. https://doi.org/10.1007/s10021-010-9402-x.

McClain, M.E., Boyer, E.W., Dent, C.L., Gergel, S.E., Grimm, N.B., Groffman, P.M., Hart, S.C., Harvey, J.W., Johnston, C.A., Mayorga, E., McDowell, W.H., Pinay, G., 2003. Biogeochemical hot spots and hot moments at the interface of terrestrial and aquatic ecosystems. Ecosystems 6, 301–312. https://doi.org/10.1007/s10021-003-0161-9.

Menon, S., Denman, K.L., Brasseur, G., Chidthaisong, A., Ciais, P., Cox, P.M., Dickinson, R.E., Hauglustaine, D., Heinze, C., Holland, E., Jacob, D., Lohmann, U., Ramachandran, S., Wofsy, S.C., Zhang, X., 2007. Couplings Between Changes in the Climate System and Biogeochemistry. Lawrence Berkeley National Lab. (LBNL), Berkeley, CA (United States). https://www.osti.gov/biblio/934721. (Accessed 26 March 2024).

Meurer, K.H.E., Franko, U., Spott, O., Stange, C.F., Jungkunst, H.F., 2016. Model testing for nitrous oxide (N2O) fluxes from Amazonian cattle pastures. Atmos. Environ. 143, 67–78. https://doi.org/10.1016/j.atmosenv.2016.08.047.

Meurer, K.H.E., Boenecke, E., Franko, U., 2019. Evaluating emissions of nitrous oxide from cropland soils under different rotations in Mato Grosso, Brazil: a scenario simulation study. Pedosphere 29, 432–443. https://doi.org/10.1016/S1002-0160(19)60812-X.

Miller, L.T., Griffis, T.J., Erickson, M.D., Turner, P.A., Deventer, M.J., Chen, Z., Yu, Z., Venterea, R.T., Baker, J.M., Frie, A.L., 2022. Response of nitrous oxide emissions to individual rain events and future changes in precipitation. J. Environ. Qual. 51, 312–324. https://doi.org/10.1002/jeq2.20348.

Molodovskaya, M., Singurindy, O., Richards, B.K., Warland, J., Johnson, M.S., Steenhuis, T.S., 2012. Temporal variability of nitrous oxide from fertilized croplands: hot moment analysis. Soil Sci. Soc. Am. J. 76, 1728–1740. https://doi.org/10.2136/sssaj2012.0039.

Ogle, S.M., Butterbach-Bahl, K., Cardenas, L., Skiba, U., Scheer, C., 2020. From research to policy: optimizing the design of a national monitoring system to mitigate soil nitrous oxide emissions. Curr. Opin. Environ. Sustain. 47, 28–36. https://doi.org/10.1016/j.cosust.2020.06.003.

Parton, W.J., Mosier, A.R., Ojima, D.S., Valentine, D.W., Schimel, D.S., Weier, K., Kulmala, A.E., 1996. Generalized model for N2 and N2O production from nitrification and denitrification. Glob. Biogeochem. Cycles 10, 401–412. https://doi.org/10.1029/96GB01455.

Parton, W.J., Hartman, M., Ojima, D., Schimel, D., 1998. DAYCENT and its land surface submodel: description and testing. Glob. Planet. Change 19, 35–48. https://doi.org/10.1016/S0921-8181(98)00040-X.

Parton, W.J., Holland, E.A., Del Grosso, S.J., Hartman, M.D., Martin, R.E., Mosier, A.R., Ojima, D.S., Schimel, D.S., 2001. Generalized model for NO x and N2O emissions from soils. J. Geophys. Res. Atmospheres 106, 17403–17419. https://doi.org/10.1029/2001JD900101.

Piani, C., Haerter, J.O., Coppola, E., 2010. Statistical bias correction for daily precipitation in regional climate models over Europe. Theor. Appl. Climatol. 99, 187–192. https://doi.org/10.1007/s00704-009-0134-9.

Posit team, 2022. Rstudio: Integrated Development Environment for R. Posit Software. PBC, Boston, MA.

R Core Team, 2022. R: a Language and Environment for Statistical Computing. R Foundation for Statistical Computing, Vienna, Austria. https://www.R-project.org/.

Roe, G., 2009. Feedbacks, timescales, and seeing red. Annu. Rev. Earth Planet Sci. 37, 93–115. https://doi.org/10.1146/annurev.earth.061008.134734.

Rychel, K., Meurer, K.H.E., Börjesson, G., Strömgren, M., Getahun, G.T., Kirchmann, H., Kätterer, T., 2020. Deep N fertilizer placement mitigated N2O emissions in a Swedish field trial with cereals. Nutr. Cycl. Agroecosystems 118, 133–148. https://doi.org/10.1007/s10705-020-10089-3.

Sang, J., Lakshani, M.M.T., Chamindu Deepagoda, T.K.K., Shen, Y., Li, Y., 2022. Drying and rewetting cycles increased soil carbon dioxide rather than nitrous oxide emissions: a meta-analysis. J. Environ. Manage. 324, 116391. https://doi.org/10.1016/j.jenvman.2022.116391.

Sillmann, J., Thorarinsdottir, T., Keenlyside, N., Schaller, N., Alexander, L.V., Hegerl, G., Seneviratne, S.I., Vautard, R., Zhang, X., Zwiers, F.W., 2017. Understanding, modeling and predicting weather and climate extremes: challenges and opportunities. Weather Clim. Extrem. 18, 65–74. https://doi.org/10.1016/j.wace.2017.10.003.

Song, X., Ju, X., Topp, C.F.E., Rees, R.M., 2019. Oxygen regulates nitrous oxide production directly in agricultural soils. Environ. Sci. Technol. 53, 12539–12547. https://doi.org/10.1021/acs.est.9b03089.

Song, X., Wei, H., Rees, R.M., Ju, X., 2022. Soil oxygen depletion and corresponding nitrous oxide production at hot moments in an agricultural soil. Environ. Pollut. 292, 118345. https://doi.org/10.1016/j.envpol.2021.118345.

Stange, F., Butterbach-Bahl, K., Papen, H., Zechmeister-Boltenstern, S., Li, C., Aber, J., 2000. A process-oriented model of N2O and NO emissions from forest soils: 2. Sensitivity analysis and validation. J. Geophys. Res. Atmospheres 105, 4385–4398. https://doi.org/10.1029/1999JD900948.

Stuchiner, E., Xu, J., Eddy, W.C., DeLucia, E.H., Yang, W.H., 2024. Hot or not? An evaluation of methods for identifying hot moments of nitrous oxide emissions from soils. https://doi.org/10.22541/essoar.171052507.72136455/v1.

Tegegne, G., Melesse, A.M., Worqlul, A.W., 2020. Development of multi-model ensemble approach for enhanced assessment of impacts of climate change on climate extremes. Sci. Total Environ. 704, 135357. https://doi.org/10.1016/j.scitotenv.2019.135357.

Thompson, R.L., Lassaletta, L., Patra, P.K., Wilson, C., Wells, K.C., Gressent, A., Koffi, E.N., Chipperfield, M.P., Winiwarter, W., Davidson, E.A., Tian, H., Canadell, J.G., 2019. Acceleration of global N2O emissions seen from two decades of atmospheric inversion. Nat. Clim. Change 9, 993–998. https://doi.org/10.1038/s41558-019-0613-7.

Vautard, R., Kadygrov, N., Iles, C., Boberg, F., Buonomo, E., Bülow, K., Coppola, E., Corre, L., van Meijgaard, E., Nogherotto, R., Sandstad, M., Schwingshackl, C., Somot, S., Aalbers, E., Christensen, O.B., Ciarlo, J.M., Demory, M.-E., Giorgi, F., Jacob, D., Jones, R.G., Keuler, K., Kjellström, E., Lenderink, G., Levavasseur, G., Nikulin, G., Sillmann, J., Solidoro, C., Sørland, S.L., Steger, C., Teichmann, C., Warrach-Sagi, K., Wulfmeyer, V., 2021. Evaluation of the large EURO-CORDEX regional climate model ensemble. J. Geophys. Res. Atmospheres 126, e2019JD032344. https://doi.org/10.1029/2019JD032344.

Vor, T., Dyckmans, J., Loftfield, N., Beese, F., Flessa, H., 2003. Aeration effects on CO2, N2O, and CH4 emission and leachate composition of a forest soil. J. Plant Nutr. Soil Sci. 166, 39–45. https://doi.org/10.1002/jpln.200390010.

Walfish, S., 2006. A review of statistical outlier methods. Pharm. Technol. 30, 82.

Wang, B., Zheng, L., Liu, D.L., Ji, F., Clark, A., Yu, Q., 2018. Using multi-model ensembles of CMIP5 global climate models to reproduce observed monthly rainfall and temperature with machine learning methods in Australia. Int. J. Climatol. 38, 4891–4902. https://doi.org/10.1002/joc.5705.

Wang, C., Amon, B., Schulz, K., Mehdi, B., 2021. Factors that influence nitrous oxide emissions from agricultural soils as well as their representation in simulation models: a review. Agronomy 11, 770. https://doi.org/10.3390/agronomy11040770.

Wei, H., Song, X., Liu, Y., Wang, R., Zheng, X., Butterbach-Bahl, K., Venterea, R.T., Wu, D., Ju, X., 2023. In situ 15N-N2O site preference and O2 concentration dynamics disclose the complexity of N2O production processes in agricultural soil. Glob. Change Biol. 29, 4910–4923. https://doi.org/10.1111/gcb.16753.

Xing, H., Smith, ChrisJ., Wang, E., Macdonald, B., Wårlind, D., 2023. Modelling nitrous oxide emissions: comparing algorithms in six widely used agro-ecological models. Soil Res. 61, 523–541. https://doi.org/10.1071/SR22009.

Yadav, D., Wang, J., 2021. An improved UK-DNDC model for evaluations of soil temperature and nitrous oxide emissions from Canadian agriculture. Plant Soil 469, 15–37. https://doi.org/10.1007/s11104-021-05125-2.

Yan, G., Mu, C., Xing, Y., Wang, Q., 2018. Responses and mechanisms of soil greenhouse gas fluxes to changes in precipitation intensity and duration: a meta-analysis for a global perspective. Can. J. Soil Sci. 98, 591–603. https://doi.org/10.1139/cjss-2018-0002.

Zhang, W., Liu, C., Zheng, X., Zhou, Z., Cui, F., Zhu, B., Haas, E., Klatt, S., Butterbach-Bahl, K., Kiese, R., 2015. Comparison of the DNDC, LandscapeDNDC and IAP-N-GAS models for simulating nitrous oxide and nitric oxide emissions from the winter wheat–summer maize rotation system. Agric. Syst. 140, 1–10. https://doi.org/10.1016/j.agsy.2015.08.003.

Zhang, W., Yao, Z., Li, S., Zheng, X., Zhang, H., Ma, L., Wang, K., Wang, R., Liu, C., Han, S., Deng, J., Li, Y., 2021. An improved process-oriented hydro-biogeochemical model for simulating dynamic fluxes of methane and nitrous oxide in alpine ecosystems with seasonally frozen soils. Biogeosciences 18, 4211–4225. https://doi.org/10.5194/bg-18-4211-2021.

Zhang, K., Li, M., Yan, Z., Li, M., Kang, E., Yan, L., Zhang, X., Li, Y., Wang, J., Yang, A., Niu, Y., Kang, X., 2022. Changes in precipitation regime lead to acceleration of the N cycle and dramatic N2O emission. Sci. Total Environ. 808, 152140. https://doi.org/10.1016/j.scitotenv.2021.152140.

Zhao, X., Min, J., Wang, S., Shi, W., Xing, G., 2011. Further understanding of nitrous oxide emission from paddy fields under rice/wheat rotation in south China. J. Geophys. Res. Biogeosciences 116. https://doi.org/10.1029/2010JG001528.